ChemBioChem

Research Article
doi.org/10.1002/cbic.202500660

Chemistry Europe
European Chemical Societies Publishing

www.chembiochem.org

Introducing Quantitative Assessment of Michaelis Constant (K_m) Accuracy

Tong Ye Wang, Parmeetpal Dhillon, Svetlana M. Krylova, Amit Bijlani, Sebastian Schreiber, Dasantila Golemi-Kotra, Joachim Jose, and Sergey N. Krylov*

The Michaelis constant (K_m) is central to enzyme kinetics, guiding variant selection, inhibitor screening, and metabolic modeling. However, K_m obtained by nonlinear regression can be substantially inaccurate even when the reported standard error (SE) appears small. Common software reports SE but provides no accuracy metric. This gap is addressed by extending the accuracy confidence interval (ACI) framework to K_m (ACI-K_m) through a binding-isotherm formulation of the velocity–substrate fit. Given confidence intervals for concentration accuracy, the method quantifies how residual systematic uncertainties in enzyme and substrate concentrations (E_0 and S_0) propagate into the determined K_m values and provides a probabilistic interval expected to enclose the accurate value. The approach requires no additional kinetic experiments and is directly applicable to existing datasets. Concentration-accuracy intervals can be estimated from calibration data, reagent specifications, or quality-control records. ACI-K_m is valid across a wide range of E_0/K_m conditions, including relatively high E_0. A free web application (https://aci.sci.yorku.ca) implements ACI-K_m. Tests on synthetic and experimental datasets show that $K_m \pm$ SE can severely underestimate uncertainty, whereas ACI provides more reliable accuracy bounds for decision-making, complementing rather than replacing traditional precision metrics by providing quantitative diagnostic bounds for concentration-related uncertainties in K_m determination.

1. Introduction

Enzymatic reactions are fundamental to biochemical transformations requiring catalysis, typically proceeding through an intermediate enzyme–substrate complex. Michaelis constant (K_m), a key parameter characterizing enzymatic activity, provides insights into enzyme–substrate affinity and reflects the stability of the intermediate complex under the quasisteady-state approximation (QSSA).[1–3]

This work focuses on the accuracy of K_m. Accuracy reflects how close the determined parameter is to the true, model-implied value, whereas precision refers to the statistical scatter of a parameter estimate, e.g., the standard error (SE) returned by nonlinear regression. Crucially, a parameter can be highly precise but grossly inaccurate if systematic errors bias the measurement. Thus, ensuring not only precision but also the accuracy of parameters such as K_m is essential for meaningful biochemical interpretations and sound decision-making.

Reliable K_m values are critical across diverse biochemical applications. Because K_m guides variant ranking, inhibitor and substrate concentrations in assays, metabolic-flux modeling, and bioprocess feed strategies, the accuracy (not merely the precision) of K_m is decisive for downstream decisions. In industrial biotechnology, accurate K_m values enable optimal enzyme selection, improving production efficiency and reducing costs.[4] In drug development, accurate K_m determination is vital for designing effective enzyme inhibitors and accurately modeling drug metabolism, affecting efficacy and dosage.[5–8] Similarly, biopharmaceutical enzyme dosing relies directly on accurate K_m values.[9] In metabolic engineering, accurate K_m parameters guide the optimization of metabolic fluxes and minimize pathway bottlenecks.[10] Environmental biotechnology depends on accurately known K_m values to match enzyme activity to pollutant concentrations for effective bioremediation.[11] Accurate K_m values in the food and beverage industry ensure precise control of enzymatic processes, maintaining product consistency and quality.[12,13] Overall, accurate K_m values are essential for reliable

T. Y. Wang, P. Dhillon, S. M. Krylova, A. Bijlani, S. N. Krylov
Department of Chemistry
York University
Toronto M3J 1P3, Ontario, Canada
E-mail: skrylov@yorku.ca

T. Y. Wang, P. Dhillon, S. M. Krylova, A. Bijlani, D. Golemi-Kotra, S. N. Krylov
Centre for Research on Biomolecular Interactions
York University
Toronto M3J 1P3, Ontario, Canada

S. Schreiber, J. Jose
Institute of Pharmaceutical and Medicinal Chemistry
University of Münster
48149 Münster, Germany

D. Golemi-Kotra
Department of Biology
York University
Toronto M3J 1P3, Ontario, Canada

Supporting information for this article is available on the WWW under https://doi.org/10.1002/cbic.202500660

decision-making, underscoring the practical importance of rigorous K_m accuracy assessment. To concretely demonstrate how inaccurate K_m values impact such decisions, we quantitatively explore representative practical consequences using synthetic data in the first section of Results.

Because accuracy can be assessed only against a known reference, we first clarify how synthetic and experimental data serve different purposes in this study. Validation of numerical accuracy requires comparison to a known ground truth, which can be achieved only with synthetic datasets where the kinetic parameters (K_m, k_1, k_{-1}, k_2) are defined by construction.[14] Real enzyme–substrate systems lack such known references, so experimental results can demonstrate workflow and feasibility under realistic conditions, but cannot validate accuracy or generality.

The current standard for determining K_m is the nonlinear regression of the Michaelis–Menten (MM) plot, which graphically represents the relationship between the initial reaction velocity (v_0) and the initial substrate concentration (S_0) under the standard QSSA (sQSSA).[15–17] Nonlinear regression fits the MM equation to experimental data, allowing for the estimation of both K_m and either the maximum reaction velocity ($v_{0,max}$) or the catalytic turnover rate (k_2), each accompanied by SE.[2] Typically, experimentally determined K_m values ($K_{m,det}$) are reported as "$K_{m,det} \pm \sigma$", where σ represents the SE obtained from curve fitting. This defines the precision confidence interval (PCI), such that the PCI corresponds to $[K_{m,det} - \sigma, K_{m,det} + \sigma]$ for a 68.3% confidence level.[18–20] While PCI quantifies precision, it provides no information about accuracy, leaving researchers unaware of potentially critical systematic errors. Standard software tools (e.g., GraphPad Prism and Origin) only return $K_{m,det} \pm \sigma$, and provide no direct measure of accuracy.

Significant discrepancies are frequently reported between independently determined K_m values for identical enzyme–substrate pairs under similar conditions, often with nonoverlapping PCIs.[21,22] These differences reveal the vulnerability of K_m determination to inaccuracies stemming from systematic concentration uncertainties or other experimental biases, factors not reflected in precision metrics alone. Currently, no practical, easy-to-use tool is available to quantitatively assess these systematic errors without requiring additional experimentation, leaving critical risks of misinterpretation and incorrect decision-making unaddressed.

We recently introduced the concept of the accuracy confidence interval (ACI), a quantitative metric addressing systematic errors by using a correctly chosen regression model as the reference standard instead of the inherently unknowable true value of a parameter.[18] Assuming that all correctable systematic errors have been rigorously minimized, the ACI represents the interval arising from unavoidable residual systematic uncertainties (in concentrations and measured signals), bounded by two calculated values, within which the true parameter value is expected to lie with a defined probability. These bounds are obtained by combining error propagation and regression stability analyses.[18] The validity of the conversion between random errors of variables and confidence intervals (CIs) of systematic errors depends on adherence to certain experimental protocols and assumptions concerning the preparation of stock solutions.[18,23] For example, random errors in preparing stock solutions may propagate as systematic concentration errors when a single set of stock solutions is used to prepare all dilutions for the parameter-determination experiment.

In our earlier work, we demonstrated the ACI concept by developing a workflow for computing the ACI of equilibrium dissociation constants (K_d) for affinity complexes.[18,23,24] During a similar error-propagation analysis for K_m determination, we uncovered an overlooked mathematical identity: under QSSA, K_m determination is mathematically equivalent to K_d determination. Thus, the comprehensive ACI workflow developed for K_d[18] is fully applicable to K_m determination upon straightforward renaming of variables: ligand → enzyme, target → substrate, and $K_d \rightarrow K_m$. This insight represents a valuable unification, enabling a compact and universally applicable treatment of K_m accuracy. This approach does not add computational complexity and allows rigorous quantitative assessment of K_m accuracy with no additional kinetic experiments beyond standard MM assays.

Importantly, the binding-isotherm regression model assumes that $v_{0,max}$ can be reliably determined experimentally. Thus, our approach is primarily suited to enzymatic reactions that exhibit saturation in MM plots. Under such conditions, the experimentally measured $v_{0,max}$ approximates the true $v_{0,max}$, thereby improving the accuracy and precision of K_m determination by reducing the number of unknown parameters from two to one.[25,26]

To ensure practical relevance and robustness, we benchmark our ACI-based method rigorously against standard nonlinear regression software (Origin), comparing K_m intervals and demonstrating that our approach reliably captures systematic errors overlooked by conventional PCI-based analyses. To facilitate rapid and widespread adoption of this accuracy assessment tool, we integrated K_m ACI calculations into a freely accessible, user-friendly web application (https://aci.sci.yorku.ca). The combined quantitative assessment of K_m accuracy and precision will improve the reliability of enzymatic studies and reduce the risk of inaccuracies adversely influencing biochemical research and industrial decision-making.

2. Results

2.1. Practical Consequences of Inaccurate K_m Values

The research community often underestimates the importance of K_m accuracy because i) K_m is viewed as an estimated parameter under QSSA, and thus its accuracy is dismissed on the grounds that the parameter lacks a "true" value or exists only at an unknown time point; ii) small SEs are routinely misinterpreted as evidence of correctness, iii) popular analysis software such as GraphPad Prism and Origin report precision but not accuracy, iv) teaching and practice have traditionally emphasized replicate scatter over bias, v) there has been no user-friendly method to quantify systematic uncertainty until now, and vi) researchers

often rely on relative K_m comparisons, assuming that systematic errors cancel out across variants.

However, the precondition of any meaningful scientific measurement or parameter determination is the existence of a true (or most accurate attainable) value; otherwise, the measurement itself is meaningless, and K_m is no exception. In K_m determination, we adopt the QSSA as a working assumption, even though its applicability may not be absolute, and then seek to achieve the highest possible accuracy of the determined K_m. Critically, the systematic uncertainties of all experimental variables should be considered during K_m determination, but this is often (if not always) neglected in conventional data analysis. Traditional studies typically rely on single-point "mean" values to rank enzymes, even though such values can differ substantially and, in some cases, even reverse rank orders. To highlight these issues, the first section of our results is dedicated to demonstrating the practical consequences of relying on conventionally determined but inaccurate K_m values.

Accurate determination of K_m is not merely an academic concern but a practical necessity, as it directly influences a wide range of downstream decisions in biochemistry, systems biology, and industrial biotechnology. To illustrate how even moderate systematic errors in experimental variables can lead to significant practical consequences, we generated fully synthetic progress curves by imposing 20% systematic errors on both the initial enzyme and substrate concentrations (E_0 and S_0), using systems with known true kinetic parameters by design. All simulations were performed within the standard quasi-steady-state regime assumed by the MM model, ensuring that the observed effects reflect systematic-error propagation rather than pre-steady-state kinetics. The resulting MM plots were then fitted using the classical MM equation and standard least-squares (L-S) regression in Python, functionally equivalent to the fitting procedures implemented in GraphPad Prism and Origin. From these fits, the $K_{m,det}$ value, and the maximum initial reaction velocity ($v_{0,max}$) were simultaneously obtained, allowing the calculation of the catalytic rate constant k_2. See Note S1 in the Supporting Information for further details of this virtual study.

Most screening and ranking campaigns prioritize catalytic efficiency (k_2/K_m) as the ranking metric, typically without accounting for uncertainty, rather than evaluating K_m alone.[27] Following this industry standard, ten synthetic enzymes were designed to display a fivefold spread in true catalytic efficiency (0.043 – 0.200 $\mu M^{-1} s^{-1}$), and the enzymes would exhibit a true monotonic rank order. Upon using L-S regression to fit the MM curves, the determined apparent catalytic efficiencies collapsed into a narrow 0.033 – 0.039 $\mu M^{-1} s^{-1}$ range, and the ranking reversed almost completely (**Figure 1**A). This distortion arose because the relative systematic error in the determined K_m increases with the ratio of the true initial enzyme concentration (E_0) to the true K_m value (Figure 1B). As a result, the genuine top performer (Pair 01) fell to ninth place, while a mid-field variant (Pair 04) surfaced as the apparently most efficient enzyme. Notably, the assay employed the canonical substrate concentration range of (0.1–10)×K_m and confirmed linear initial-rate segments with ≤10% substrate depletion, ruling out poor experimental design as the cause. In a real screening campaign, such rank-order reversals could misdirect resources toward underperforming

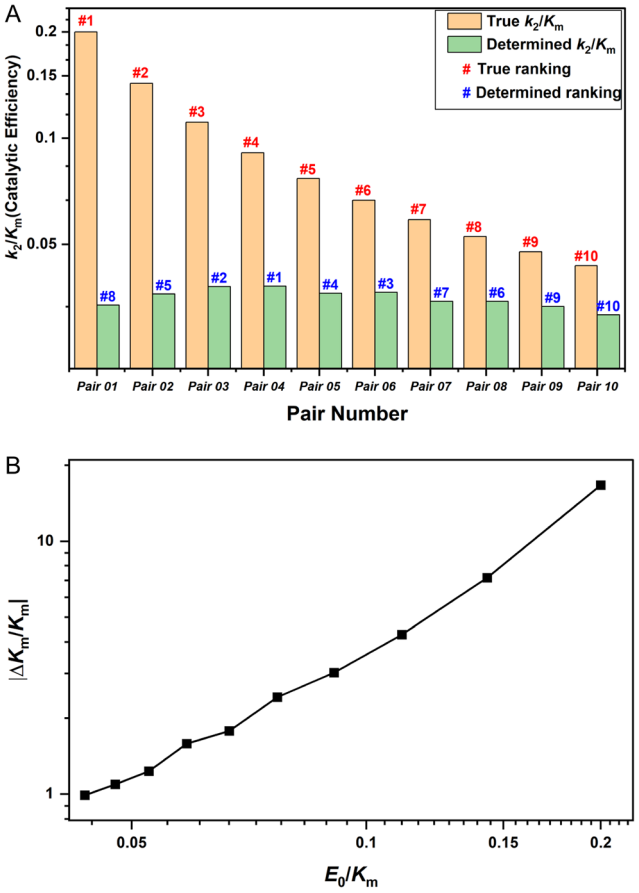

Figure 1. Impact of conventional L-S regression on catalytic efficiency ranking and $K_{m,\ det}$ accuracy. A) True (orange) versus determined (green) catalytic efficiencies (k_2/K_m) for ten synthetic enzyme–substrate pairs. True and determined rankings are labeled in red and blue, respectively (#1 = highest efficiency). Despite a fivefold spread in true efficiencies, L-S regression compressed the apparent values and severely distorted the rank order. B) Log–log plot of the relative systematic error in $K_{m,\ det}$ ($|\Delta K_m/K_m|$) as a function of true E_0/K_m, illustrating that $K_{m,\ det}$ inaccuracy increases steeply with rising the true initial enzyme concentration (E_0) relative to the true value of K_m.

catalysts and prematurely eliminate high-value candidates, costly missteps for both academia and industry.

We propose that the previously introduced ACI framework,[18] originally developed to assess K_d accuracy, can serve as a critical checkpoint for identifying the higher limit of K_m accuracy. By quantifying potential bias in advance, ACI can alert practitioners when variant rankings may be unreliable because the experimental conditions fall outside an accuracy-safe regime, thereby enabling methodological adjustments before consequential downstream decisions are made.

2.2. Mathematical Framework of K_m Determination and its Analogy to K_d Determination

The mathematical framework underlying the classical determination of K_d through L-S nonlinear regression of a binding isotherm has been thoroughly described in our previous work (Wang et al., 2024).[23] In the present study, we extend this analysis by

exploring the parallels between the mathematical approaches used for determining K_m and K_d.

To formalize the mathematics of K_m determination, we consider a classic mechanism of enzymatic reaction

$$E + S \underset{k_{-1}}{\overset{k_1}{\rightleftharpoons}} C \xrightarrow{k_2} E + P \tag{1}$$

where E is the enzyme, S is the substrate, C is the intermediate enzyme–substrate complex, and P is the product, while k_1, k_{-1}, and k_2 are the rate constants for complex formation, complex dissociation, and catalytic turnover, respectively.[21] This mechanism assumes that product formation is the rate-limiting step and that the initial reaction velocity (v_0) is measured under conditions where product accumulation is minimal and substrate depletion is negligible. Under these conditions, v_0 can be expressed as $v_0 = k_2C$, where C is the concentration of the enzyme–substrate complex.[21,28,29]

In the quasi-steady state, the rates of formation and consumption of C are considered equal, so that the net rate of change in the total complex concentration is zero

$$\frac{dC}{dt} = k_1ES - (k_2 + k_{-1})C = 0 \tag{2}$$

From this equation, K_m is defined as

$$K_m = \frac{k_2 + k_{-1}}{k_1} = \frac{ES}{C} \tag{3}$$

which is mathematically analogous to the definition of K_d.[23]

Under the conditions where v_0 is measured (i.e., when the amount of the product formed is negligible), the mass balance for the total concentrations of enzyme and substrate can be expressed as

$$\begin{aligned} E + C &= E_0 \\ S + C &= S_0 \end{aligned} \tag{4}$$

where E_0 is the total enzyme concentration and S_0 is the total substrate concentration.

Let us introduce the fraction R of free enzyme, which is mathematically analogous to the fraction of free ligand used in K_d determination

$$R = \frac{E}{E_0} \tag{5}$$

Using the definitions of K_m and R ((Equation 3) and (5)) as well as mass balance Equations (Equation 4), we can link K_m to S_0, E_0, and R

$$K_m = \frac{S_0 - E_0(1 - R)}{(1/R - 1)} \tag{6}$$

This expression parallels the single-point K_d-determination equation employed in classic equilibrium approaches.[23]

In enzymatic reactions, researchers typically measure v_0. We can express v_0 as the reaction rate (dP/dt) at the beginning of the quasi-steady state and link R with the reaction velocity

$$\begin{aligned} v_0 &= \frac{dP}{dt} = k_2C = k_2E_0(1 - R) = v_{0,\max}(1 - R) \Rightarrow \\ R &= \frac{v_{0,\max} - v_0}{v_{0,\max}} \end{aligned} \tag{7}$$

here, $v_{0,max}$ denotes the maximum initial reaction velocity, which theoretically equals k_2E_0. This expression for the determination of R in enzymatic reactions is analogous to the equation used for determining the fraction of unbound ligand in K_d determination.[23]

Finally, (Equation 6) can be rewritten as a quadratic equation for R and solved to yield a theoretical dependence of R on K_m, S_0, and E_0

$$R = -\frac{K_m + S_0 - E_0}{2E_0} + \sqrt{\left(\frac{K_m + S_0 - E_0}{2E_0}\right)^2 + \frac{K_m}{E_0}} \tag{8}$$

This completes the mathematical formulation for finding $K_{m,det}$ by nonlinear regression of a "binding isotherm". The binding isotherm describes the dependence of R determined with (Equation 7) on S_0 for a constant E_0. The determination of $K_{m,det}$ by nonlinear regression of a binding isotherm with (Equation 8), referred to here as the "binding-isotherm model", is schematically depicted in **Figure 2**A.

2.3. The Value of Unifying the Mathematical Frameworks for K_m and K_d Determination

It is instructive to emphasize that the equilibrium of ligand–target binding and the pseudoequilibrium of enzymatic catalysis (Equation 1) are distinct processes. Despite this fundamental difference, the mathematical frameworks used to determine K_m and K_d exhibit strong analogies. A universal nonlinear regression binding-isotherm model (e.g., (Equation 8)) can be used to fit the experimental binding isotherms. Some previous studies have recognized the use of the binding-isotherm model (or its variants) for K_m determination under total QSSA (tQSSA), particularly when high enzyme concentrations (E_0) are used.[30–33] However, to the best of our knowledge, no systematic study has comprehensively examined the parallels between K_m and K_d determinations across their theoretical foundations, experimental implementations, and data analysis methodologies.

We would like to emphasize that the methodological significance of the analogous mathematics underlying K_m and K_d determinations should not be overstated. This mathematical similarity nonetheless offers a valuable unifying framework for the quantitative analysis of both binding and catalytic processes. It facilitates a streamlined, cross-disciplinary analytical approach. Notably, the binding-isotherm model (Equation 8) describes the dependence of a unitless variable, R, on substrate concentration (S_0), in contrast to conventional kinetic models that express the dependence of initial reaction velocity v_0 (dP/dt) on S_0 under either sQSSA or tQSSA. By avoiding the need to convert the instrument signal (e.g., absorbance) into product concentration (P), the binding-isotherm model simplifies the experimental workflow of K_m determination by eliminating the calibration step. Demonstrating that the

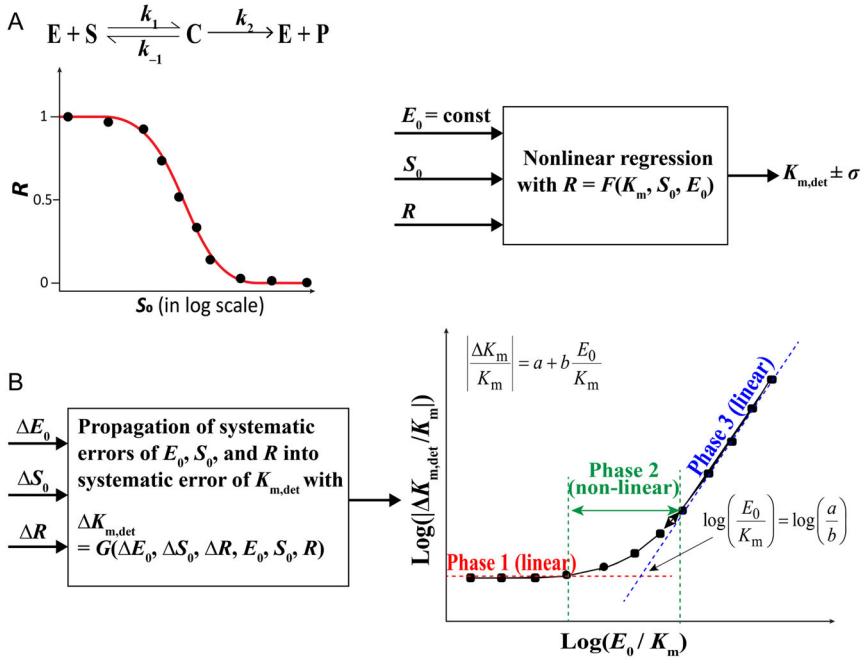

Figure 2. Schematic representations of A) determination of $K_{m,\ det}$ and its standard deviation (σ) by nonlinear regression with three variables from the binding isotherm (E_0, S_0, and R) and B) propagation of systematic errors in these variables leading to a triphasic dependence of the relative systematic error in $K_{m,\ det}$ on the ratio E_0/K_m in which K_m designates its true unknown value. (This figure is modified with permission from ref. [23] Copyright American Chemical Society).

binding-isotherm model is applicable to both K_m and K_d determinations, we offer a versatile tool that enhances the reliability of nonlinear regression analyses across diverse biochemical applications.

This consistency in mathematical treatment simplifies the validation and comparison of experimental results, as the same regression model can be employed without modification. Moreover, it allows for the direct transfer of computational tools and error-propagation techniques between studies focusing on enzymatic reactions and affinity binding, fostering greater efficiency and accuracy in biochemical research.

This unified approach also aids in the education and training of researchers by reducing the learning curve and minimizing the potential for methodological errors. Mastering a single robust model enhances efficiency and ensures consistency across studies. Ultimately, identical mathematics enables advancements in one area of study to be readily adapted to others, accelerating innovation and improving the overall robustness of biochemical analyses. Here, we capitalize on the ability to directly transfer previously obtained error-propagation results and approaches for accuracy assessment from K_d to K_m.

2.4. Propagation of Systematic Errors in K_m Determination

The error propagation for K_d has been reported previously.[24] Given the mathematical similarity between K_d and K_m determinations using the binding-isotherm model, these findings can be readily adapted to K_m through a straightforward substitution of terms: replacing T_0 with S_0, L_0 with E_0, and K_d with K_m. The results of this adaptation are detailed below.

When the QSSA holds, the accuracy of $K_{m,det}$ depends on the accuracy of E_0, S_0, and R. If these values were exact (i.e., free from systematic errors), K_m determination would be accurate and subject only to random errors. However, in practice, systematic errors in E_0, S_0, and R (denoted as ΔE_0, ΔS_0, and ΔR) contribute to the systematic error in $K_{m,det}$ (denoted as ΔK_m), as explained below using an assumption that ΔE_0, ΔS_0, and ΔR are known.

The translation of ΔE_0, ΔS_0, and ΔR into ΔK_m follows error propagation rules. These rules vary depending on whether ΔE_0, ΔS_0, and ΔR are strongly or weakly correlated. If they are fully correlated (which occurs when similar procedures are used for enzyme and substrate solution preparation, and ΔR results solely from ΔE_0 and ΔS_0), the absolute value of ΔK_m can be approximated as

$$|\Delta K_m| = \left|\left(\frac{\partial K_m}{\partial S_0}\right)\Delta S_0\right| + \left|\left(\frac{\partial K_m}{\partial E_0}\right)\Delta E_0\right| + \left|\left(\frac{\partial K_m}{\partial R}\right)\Delta R\right| \quad (9)$$

Applying this relationship to the dependence of K_m on E_0, S_0, and R ((Equation 6)) gives (Note S2, Supporting Information)

$$\left|\frac{\Delta K_m}{K_m}\right| = a + b\frac{E_0}{K_m} \quad (10)$$

where a and b are error-dependent coefficients: a is determined by the relative systematic errors in substrate concentration and response signal, i.e., $|\Delta S_0/S_0|$ and $|\Delta R/R|$, while b also incorporates the relative systematic error in enzyme concentration, $|\Delta E_0/E_0|$, making it a function of all three error terms.

If ΔE_0, ΔS_0, and ΔR are weakly correlated (e.g., when enzyme and substrate solutions are prepared using different approaches,

and ΔR is independent of ΔE_0 and ΔS_0), the absolute value of ΔK_m can be approximated as (Note S2, Supporting Information)

$$|\Delta K_m| = \sqrt{\left(\frac{\partial K_m}{\partial S_0}\right)^2 \Delta {S_0}^2 + \left(\frac{\partial K_m}{\partial E_0}\right)^2 \Delta {E_0}^2 + \left(\frac{\partial K_m}{\partial R}\right)^2 \Delta R^2} \quad (11)$$

Applying this relationship to (Equation 6) gives

$$\left|\frac{\Delta K_m}{K_m}\right| = \sqrt{\alpha^2 + \lambda \frac{E_0}{K_m} + \beta^2 \left(\frac{E_0}{K_m}\right)^2} \quad (12)$$

where α, λ, and β are error-dependent coefficients. Both α and λ depend solely on $|\Delta S_0/S_0|$ and $|\Delta R/R|$, while β depends on all three relative errors: $|\Delta S_0/S_0|$, $|\Delta E_0/E_0|$ and $|\Delta R/R|$. (Equation 10) and (12) were obtained with a single simplifying assumption: the value of R determined from measured initial reaction velocities (Equation 7) is equal to 0.5, leading to the least erroneous $K_{m,det}$.[18,34] Thus, (Equations 10) and (12) represent the lower limit for relative systematic errors in $K_{m,det}$. Exact dependencies of a and b, as well as α, λ, and β on $|\Delta S_0/S_0|$, $|\Delta E_0/E_0|$, and $|\Delta R/R|$, which can be found elsewhere (and in Note S2, Supporting Information),[24] are not required for our analysis here.

(Equation 10) and (12) share a triphasic shape for the dependence of $|\Delta K_m/K_m|$ on E_0/K_m, as illustrated in double-log coordinates (Figure 2B). In the first phase, at low E_0/K_m values, an "insensitive region" emerges in which $|\Delta K_m/K_m|$ shows negligible dependence on E_0/K_m. This behavior arises because the leading term in (Equation 10) and the first term under the square root in (Equation 12) dominate the overall error expression. In the third phase, at high E_0/K_m values, a "highly sensitive region" appears, where $|\Delta K_m/K_m|$ increases linearly with E_0/K_m ($|\Delta K_m/K_m| = b(E_0/K_m)$ and $|\Delta K_m/K_m| = \beta(E_0/K_m)$, respectively). Between these two extremes lies a nonlinear transition region connecting the insensitive and highly sensitive phases.

It is important to note that these error-propagation analyses assume K_m is the sole parameter being determined. However, conventional MM curves typically estimate both K_m and $v_{0,max}$ (or k_2) simultaneously, as was done in the synthetic ranking simulations (Figure 1). While the resulting error trends may differ between the single-parameter and two-parameter cases, the results in Figure 1 clearly demonstrate that simultaneous fitting of both parameters does not improve K_m accuracy, and may in fact worsen it.

Both (Equation 10) and (12) indicate that minimizing $|\Delta K_m/K_m|$ involves reducing enzyme concentration E_0 (to lower the E_0/K_m ratio) and minimizing relative systematic errors in E_0, S_0, and R. However, decreasing E_0 is constrained by the instrument's limit of quantitation (LOQ) for the product of the enzymatic reaction.[35] Below this limit, excessively long times are required to accumulate sufficient product for reliable v_0 measurement, crucial for accurate calculation of R with (Equation 7) . Moreover, systematic errors in concentrations cannot practically be reduced below the random errors associated with stock-solution preparations across different samples.[18,23] These limitations render highly accurate K_m determination inherently challenging, underscoring the importance of quantitative methods for assessing the accuracy or systematic uncertainty of $K_{m,det}$. Given the mathematical analogy between K_d and K_m determinations, the error-assessment framework previously developed for K_d can be directly applied to K_m, as demonstrated below.

2.5. Quantitative Assessment of K_m Accuracy by Computing its ACI

In general, accuracy is a quantitative term associated with a systematic error, which is defined as the deviation of the determined value from the true value. When the true value is fundamentally unknown, the systematic error cannot be calculated from this definition. As a result, accuracy assessment becomes a complex problem, even for parameters measurable against reference standards like length, mass, time, charge, and temperature.[36–39] This challenge is even more pronounced for parameters without reference standards, such as K_d and K_m, which remain constant only under strictly defined conditions or within specific time intervals.[40–44]

We recently suggested an approach to overcome this issue by introducing an ACI for parameters determined using correct regression models. In this concept, the correct regression model replaces the true value of the parameter as a reference standard.[18] The ACI defines a range within which the true value lies with a specified probability. For certain regression models, the bounds of this range can be computed by combining error-propagation and regression-stability analyses, provided that CIs for systematic errors in variables can be experimentally estimated.[18] Together, these two approaches constitute the complementary pillars of calculating the ACI of K_m.

2.6. Error-Propagation Analysis

The error-propagation analysis begins by transforming random errors in variables (e.g., concentrations) into CIs for their systematic errors. Error-propagation rules are then applied to identify the systematic-error boundaries (of variables) defining the ACI of the sought parameter.[18]

Although random and systematic errors are generally distinct concepts, in typical experimental protocols for K_d and K_m determinations, CIs for systematic concentration errors can be estimated based on the observed random errors across independently prepared stock solutions.[18,23] Specifically, this conversion relies on the assumption that all "true" systematic errors in experimental variables, focusing here on concentrations, have been effectively eliminated through rigorous experimental procedures such as calibrating volume and mass measurement devices, correcting for reagent impurities, and eliminating adsorption effects.[23] In this context, random errors introduced during stock solution preparation propagate as systematic errors in the final samples and define the CIs for systematic concentration errors, since the same stock solutions are used for all dilutions in K_d or K_m determinations, which is a common experimental practice.[45,46]

Given the similarity between K_d and K_m determinations, the approaches outlined in our recent K_d-focused study can be applied to minimize $|\Delta S_0/S_0|$ and $|\Delta E_0/E_0|$.[23] When such errors are minimized, it is reasonable to approximate the CIs of $|\Delta S_0/S_0|$ and $|\Delta E_0/E_0|$ using the relative random errors in stock-solution concentrations (i.e., $\delta S_0/S_0$ and $\delta E_0/E_0$).[18,23] The values of $\delta S_0/S_0$ and $\delta E_0/E_0$ can be experimentally determined based on the spectroscopic signals (e.g., light absorption) from substrate and enzyme across multiple independent stock solution preparations, which involves only modest additional effort. Alternatively, they can be estimated based on the accuracy uncertainties of the reagent purity and the equipment used for sample preparation, requiring no additional experimental work. Regardless of the chosen approach, the experimental effort involved in assessing concentration-related systematic errors within the ACI framework is minimal compared to that required for conventional K_m systematic uncertainty assessments, which often rely on additional kinetic assays.

Since no established method quantitatively assesses the CIs of $\Delta R/R$, here we only consider the CIs of $\Delta S_0/S_0$ and $\Delta E_0/E_0$ to compute the narrower limit of the ACI of K_m. Notably, this procedure should be applied after minimizing the underlying systematic errors in the experimental signals, such as those from instrument calibration or baseline selection, which must be strictly and routinely controlled. By applying the error-propagation rules ((Equation 10) or (12)) to a specific case of (Equation 6) (e.g., $R = 0.5$), we can obtain the $\Delta S_0/S_0$ and $\Delta E_0/E_0$ values (within their corresponding CIs) that together define the CI of $\Delta K_m/K_m$ at specified probabilities (Note S3, Supporting Information).

2.7. Regression-Stability Analysis

The regression-stability analysis quantitatively evaluates the stability of the $K_{m,det}$ value to changes in E_0 used in nonlinear regression. This process first computes the CI of E_0/K_m and subsequently determines the ACI of K_m.

Traditionally, researchers qualitatively confirm the accuracy of $K_{m,det}$ by experimentally examining whether $K_{m,det}$ is insensitive to changes in E_0 in multiple MM plots.[47] However, this approach is time-consuming, resource-intensive, and lacks quantitative rigor. Inspired by the mathematical similarity between K_d and K_m determinations, we developed a quantitative regression-stability analysis, integrated with error propagation, to derive the ACI of K_m from a single binding isotherm ("R vs S_0"), which can be fitted using the binding-isotherm model (Equation 8).

We name this approach ACI-Km; the step-by-step conceptual workflow for ACI-Km is shown in **Figure 3**. ACI-Km requires a full MM plot ("v_0 vs S_0") obtained under QSSA. In this case, $v_{0,max}$ is experimentally achieved at the highest S_0. Using $v_{0,max}$, and Equation (7), R values for each S_0 are calculated to construct the binding isotherm ("R vs S_0"). In this study, owing to the absence of an established method to quantitatively assess the CIs of $\Delta R/R$, we restrict the application of ACI-Km to concentration-related systematic errors.

Since the effectiveness of ACI-Km depends on the regression-stability test, which requires sufficient sensitivity of $K_{m,det}$ to variations in E_0 during fitting, this approach is most reliable when the lower bound of the measured CI for E_0/K_m exceeds 0.001. When the true E_0/K_m falls below this threshold, a condition that is experimentally common in many K_m-determination

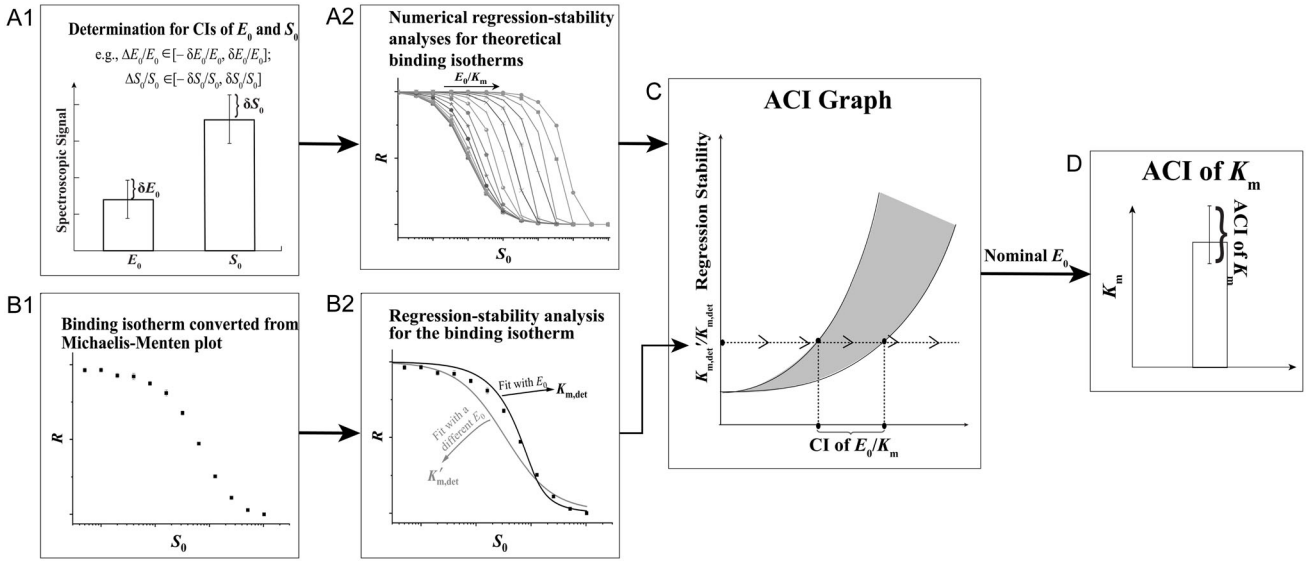

Figure 3. Conceptual workflow for computing the ACI of K_m: A1) Determine the confidence intervals (CIs) of relative systematic errors for enzyme and substrate concentrations by measuring the spectroscopic signals of enzyme and substrate stock solutions from multiple preparations. A2) Perform a numerical analysis of the regression stability of theoretical binding isotherms, incorporating the determined CIs of concentrations, over a wide range of E_0/K_m ratios. B1) Construct a binding isotherm ("R vs S_0") based on the experimental MM plot ("v_0 vs S_0"). B2) Analyze the regression stability of the binding isotherm developed in Step B1. C) Create an ACI graph of "regression stability vs E_0/K_m" using the results from Step A2, then apply the regression stability obtained in Step B2 to the graph to determine the CI of the E_0/K_m ratio. D) Use the CI of the E_0/K_m ratio and the nominal E_0 value to calculate the ACI of K_m.

experiments, the contribution of E_0 to K_m determination becomes negligible.[19] In such cases, the ACI of K_m is instead defined by the CI of S_0. This conclusion will be further validated in the program verification section.

2.8. ACI Graphs and Practical Implications

In ACI-Km, we numerically analyze the stability of $K_{m,det}$ against variations in E_0 used for nonlinear regression, based on theoretical binding isotherms generated by (Equation 8) over a wide range of E_0/K_m. The resulting graph, which depicts the dependence of regression stability on E_0/K_m, is referred to as an ACI graph (Figure 3C). Importantly, when incorporating experimentally determined CIs for the relative systematic errors in concentrations, the relationship between regression stability and E_0/K_m is represented as an area rather than a single line, as shown by the gray region in the ACI graph (Figure 3C). For a binding isotherm derived from an experimental MM plot ("v_0 vs S_0"), its regression stability can be calculated for the same E_0 variations used to construct the ACI graph. By plotting the experimental regression stability onto the ACI graph, we can determine the CI for E_0/K_m, which is then used to compute the ACI of K_m (Figure 3C,D). Because only systematic concentration uncertainties are considered here, the resulting ACI corresponds to its narrower limit.

2.9. Advancement of Graphical Approach

Although several well-established strategies based on Monte Carlo or Bayesian analysis exist for numerical error propagation in K_m determination,[33,48–51] we adopt the "graphical" approach here to intuitively demonstrate how systematic errors in variables can be amplified by a factor of E_0/K_m when propagated into the systematic error of $K_{m,det}$. This visualization provides researchers with a practical framework to estimate how much lower E_0 should be to achieve the desired accuracy in $K_{m,det}$. If the lowest feasible E_0 has already been utilized, further improvements in $K_{m,det}$ accuracy may necessitate the use of an instrument with a lower LOQ for the product. Notably, the similarity between the ACI obtained using this graphical approach and that from the Monte Carlo method has been confirmed in our previous work on ACI-Kd.[18]

2.10. ACI-Km Web Application

To ensure universal accessibility for calculating the ACI of K_m, we have integrated this functionality into the ACI webapp (https://aci.sci.yorku.ca). It is important to emphasize that the primary requirement for using the webapp to compute the ACI of K_m is that $v_{0,max}$ must be experimentally achieved with an excessively high S_0. By inputting the experimentally obtained MM plot "v_0 versus S_0" into the ACI-Km webapp interface, the curve is automatically converted into a binding isotherm "R versus S_0" under the assumption that v_0 at the highest S_0 corresponds to $v_{0,max}$ (e.g., conversion from Figure S1C to Figure S1D, Supporting Information). The webapp then generates a PDF report that provides the ACI and PCI of K_m for three confidence levels: 68.3%, 95.5%, and 99.7% (e.g., Figure S2, Supporting Information). In this study, we primarily focus on the ACI and PCI at 68.3% confidence for demonstration purposes.

2.11. Verification and Demonstration of ACI-Km

In this study, we verify the ACI-Km workflow by demonstrating its ability to produce results that align with theoretical expectations. Since the true values of key parameters, such as K_m, E_0, S_0, and their associated errors, are fundamentally unknown and uncontrollable in real experimental scenarios, the data of real experiments cannot be effectively used for the verification of ACI-Km. Therefore, we utilized computer-simulated data with well-defined, controllable variables and parameters. This approach enabled us to validate the workflow's accuracy and showcase the practical application of ACI-Km. The details of the simulations and data processing are provided in Note S4 (including Figures S1 and S2, Supporting Information).

In the simulations, we defined a set of rate constants (k_1, k_{-1}, and k_2) resulting in $K_m = 1$ μM. Reaction progress curves ("P vs time") were generated for a wide range of nominal E_0 values (0.005, 0.01, 0.05, 0.1, and 0.5 μM) and a given range of nominal S_0 values (0.01, 0.033, 0.1, 0.33, 1.0, 3.3, 10, 33, 100, 333, and 1000 μM). Given that the validity of the QSSA is widely accepted when $E_0 < S_0 + K_m$,[52] we did not further increase the nominal enzyme concentration in this study. Systematic errors were introduced with two combinations: i) $\Delta E_0/E_0 = 0.2$ and $\Delta S_0/S_0 = -0.2$ and ii) $\Delta E_0/E_0 = -0.2$ and $\Delta S_0/S_0 = 0.2$. A normally distributed relative random error of 1% was applied to the product concentrations in the synthetic progress curves. Representative synthetic reaction progress curves are shown in Figure S1A, Supporting Information. The initial linear phases of the simulated progress curves were analyzed to determine the v_0 for different nominal S_0 at each nominal E_0 (e.g., Figure S1B, Supporting Information). From these data, the MM plots "v_0 vs S_0" were constructed for each E_0 and a combination of systematic errors in E_0 and S_0 (e.g., Figure S1C, Supporting Information).

The ACI-Km webapp was used to compute the PCI and ACI of K_m for each condition. As explained in our previous work,[18] to ensure that the ACI (with 68.3% confidence level) includes the true K_m, the minimum relative random errors for E_0 and S_0 should be $\delta E_0/E_0 = |\Delta E_0/E_0|/1.36$ and $\delta S_0/S_0 = |\Delta S_0/S_0|/1.36$, which leads the input $\delta E_0/E_0 = \delta S_0/S_0 = 0.2/1.36 = 0.15$. To validate the ACI-Km workflow, we entered the nominal E_0 values, the corresponding relative random errors, and the MM plots data (derived from analysis of the simulated progress curves) into the webapp (https://aci.sci.yorku.ca). If both the webapp and ACI-Km method perform as expected and there are no systematic errors in R values, the true K_m should fall at or near one of the boundaries of the computed ACI of K_m (with 68.3% confidence), depending on the specific combination of errors introduced during the simulation of progress curves.

Figure 4 summarizes the comparison between the true/input K_m and the ACI and PCI of K_m, calculated from simulated data using ACI-Km. It is important to note that the PCI at 68.3%

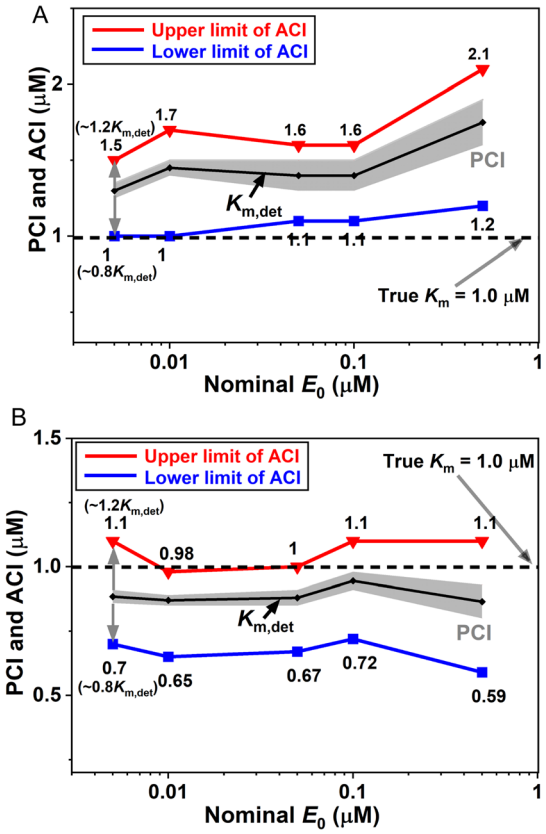

Figure 4. PCI and ACI determined using ACI-Km for two sets of MM plots derived from the simulated kinetic data under different conditions: A) $\Delta E_0/E_0 = 0.2$ and $\Delta S_0/S_0 = -0.2$, with nominal E_0 values of 0.005, 0.01, 0.05, 0.1, and 0.5 μM and B) $\Delta E_0/E_0 = -0.2$ and $\Delta S_0/S_0 = 0.2$, with nominal E_0 values of 0.01, 0.05, 0.1, and 0.5 μM. For both cases, $\delta E_0/E_0 = \delta S_0/S_0 = 0.15$ was input into the ACI web app (https://aci.sci.yorku.ca) to calculate both the ACI and PCI of K_m.

confidence corresponds to the interval $[K_{m,det} - \sigma, K_{m,det} + \sigma]$, where $K_{m,det}$ represents the determined K_m value and σ corresponds to its SE, as typically reported by software such as GraphPad Prism or Origin. The results presented in Figure 4 align well with our four theoretical predictions: i) when $E_0 << S_0 + K_m$ (e.g., $E_0/(S_0 + K_m) < 0.1$) is satisfied for all S_0 used in the simulation (i.e., $E_0 \leq 0.1$ μM), the true K_m lies near or at the boundary of the computed ACI for K_m; ii) when $E_0 > 0.1$ μM, the true K_m shifts away from the ACI boundary, likely due to difficulties in accurately measuring v_0 from the initial linear phase of the progress curve, which introduces unquantifiable systematic errors into the calculated R values[53]; iii) as E_0 increases, the ACI tends to widen due to the magnification of systematic errors, as predicted by (Equation 10) and (12) ; and iv) ACI of K_m is often much wider than PCI of K_m.

The results in Figure 4 suggest that when the condition $E_0 < S_0 + K_m$ is satisfied for all experimental S_0, and CIs for systematic errors in concentrations are accurately estimated, the ACI-Km method can compute the ACI that includes the true value of K_m. Even if this condition is not strictly met for some data points, calculating the ACI remains informative, although in this case it corresponds only to the narrower limit. A wide ACI at the experimental E_0 can serve as an indicator for experimentalists to refine their experimental conditions, such as reducing the enzyme concentration to improve accuracy. Notably, the PCI is often significantly narrower than the ACI, meaning that relying solely on the PCI can result in a substantial underestimation of the uncertainty in K_m, potentially causing inaccurate under- or overestimation of K_m. This underscores the importance of incorporating the ACI in K_m characterization to provide a more accurate representation of the true uncertainty.

Further analysis reveals that when the ratio of nominal E_0 to the true K_m was ≤ 0.01, the ACI of K_m closely matched the range from $0.8K_{m,det}$ to $1.2K_{m,det}$ (Figure 4), which could be determined solely by setting $\delta S_0/S_0 = 0.15$ while neglecting errors in E_0 (i.e., setting $\delta E_0/E_0 = 0$) (Note S5, Supporting Information). This finding suggests that for $E_0/K_m \leq 0.01$, the ACI of K_m is primarily dictated by the relative systematic error in the substrate concentration ($|\Delta S_0/S_0|$). For instance, at a 68.3% confidence level, the ACI is given by $[K_{m,det}(1–1.36\ \delta S_0/S_0),\ K_{m,det}(1 + 1.36\ \delta S_0/S_0)]$ (Note S5 and Figure S3, Supporting Information). This effect arises because, at very low E_0/K_m ratios, the contribution of the relative systematic error in E_0 ($|\Delta E_0/E_0|$) to the overall systematic error in $K_{m,det}$ becomes negligible. This behavior is evident from (Equation 10) or (12) and the corresponding expressions for the coefficients a and α provided in Note S2, Supporting Information. Furthermore, this observation suggests that while the direct calculation of ACI of K_m from the ACI graph is not feasible when the lower bound of the CI for E_0/K_m falls below 0.001 due to the limited sensitivity of $K_{m,\ det}$ to the E_0 values used in fitting, the ACI of K_m can still be estimated. Specifically, $K_{m,det}$ can be determined by fitting the binding isotherm "R versus S_0" (derived from the experimental MM plot) using (Equation 8), after which the ACI of K_m can be computed as $[K_{m,det}(1-N\delta S_0/S_0),\ K_{m,\ det}(1+N\delta S_0/S_0)]$, where N takes values of 1.36, 2.27, and 3.18 for confidence levels of 68.3%, 95.5%, and 99.7%, respectively (confirmed in Figure S3, Supporting Information).[18]

Based on these findings, we have improved the ACI-Km webapp with the following updates. When the lower bound of the CI for $E_0/K_m \geq 0.01$, the ACI of K_m is calculated using the ACI-Km workflow as shown in Figure 3. When the lower bound of the CI for $E_0/K_m < 0.01$, the ACI-Km webapp first determines $K_{m,det}$ by fitting the converted binding isotherm using (Equation 8) . The ACI of K_m is then computed using the equation above, i.e., $[K_{m,det}(1-N\delta S_0/S_0),\ K_{m,det}(1+N\delta S_0/S_0)]$. Note that, regardless of E_0/K_m, the PCI can always be calculated based on the fitted $K_{m,det}$, and its standard deviation (σ).

2.12. Application of ACI-Km to Experimental Data

After verifying and updating the ACI-Km webapp, we utilized it to evaluate the ACI and PCI of experimentally determined K_m values. To demonstrate its applicability in K_m determination, we first applied ACI-Km to a published dataset for the enzyme–substrate pair AnaAT–acetyl-coenzyme A. Additionally, we performed an experiment using lactate dehydrogenase (LDH) with pyruvate as the substrate and NADH as a co-substrate. The ACI-Km program was then employed to analyze our experimental data, further illustrating its effectiveness in estimating reliable $K_{m,det}$.

To assess the effectiveness of ACI-Km in K_m determination, we first applied it to a published dataset for the enzyme–substrate pair AnaAT–acetyl-coenzyme A from Yin et al. published in 2008.[54] This dataset represents a case where conventional MM and Lineweaver–Burk models were unsuitable, whereas the ACI-Km program based on the binding isotherm model ((Equation 8)) can provide a more accurate framework for analysis.

In the published experiment, the enzyme concentration $[AnaAT]_0$ (E_0) was 0.01 μg μl^{-1}. The molecular weight of AnaAT was determined to be 43 kDa using size-exclusion filtration, corresponding to a nominal enzyme concentration of ≈0.23 μM.[54] Substrate concentrations [acetyl-coenzyme A]$_0$ were varied at 0, 5, 10, 20, 50, 200, 500, and 1000 μM. By analyzing the product formation rate under each condition, experimental progress curves "*P* versus time" were generated, from which the MM plot "v_0 versus S_0" was established (**Figure 5**A). The MM plot was then transformed into a Lineweaver–Burk plot "$1/v_0$ versus $1/S_0$" (Figure 5B) to find $K_{m,det}$, yielding a value of 96 μM without uncertainty being reported.

The Lineweaver–Burk plot is a linearized transformation of the MM plot, which assumes $E_0 << K_m$.[47] If the E_0/K_m ratio is sufficiently small, the contribution of E_0 to K_m determination is considered negligible, resulting in an approximately linear Lineweaver–Burk plot. However, as shown in Figure 5B, the plot deviated significantly from linearity, suggesting that this assumption was not valid. This observation highlights the risks of simply assuming E_0/K_m is small enough to disregard E_0 in K_m determination without verification.

To address this limitation, we applied ACI-Km to calculate the ACI and PCI of K_m for AnaAT–acetyl-coenzyme A using the same published dataset. Unlike the conventional MM or Lineweaver–Burk approach, ACI-Km employs the binding-isotherm model ((Equation 8)), which is derived from first principles without excluding E_0 from the fitting equation. As shown in Figure 5A, the experimental MM plot approaches the plateau region at the highest substrate concentration ([acetyl-coenzyme A]$_0$ = 1000 μM), indicating that the measured v_0 at this condition was nearing $v_{0,max}$. This saturation suggests that the necessary conditions for applying the binding-isotherm model were satisfied, supporting the validity of using ACI-Km for K_m determination.

To utilize the ACI-Km program, we needed to account for the uncertainty in the accuracy of reagent concentrations. Since the original study did not report the systematic uncertainties associated with enzyme and substrate concentrations, we estimated the lower CI limits for their relative systematic errors to perform the ACI calculations. Systematic errors in enzyme concentration can arise from factors such as pipetting inaccuracies, dilution errors, sample impurities, and adsorption to surfaces, which are particularly significant at low enzyme concentrations.[55] Consequently, even under rigorous efforts to minimize these

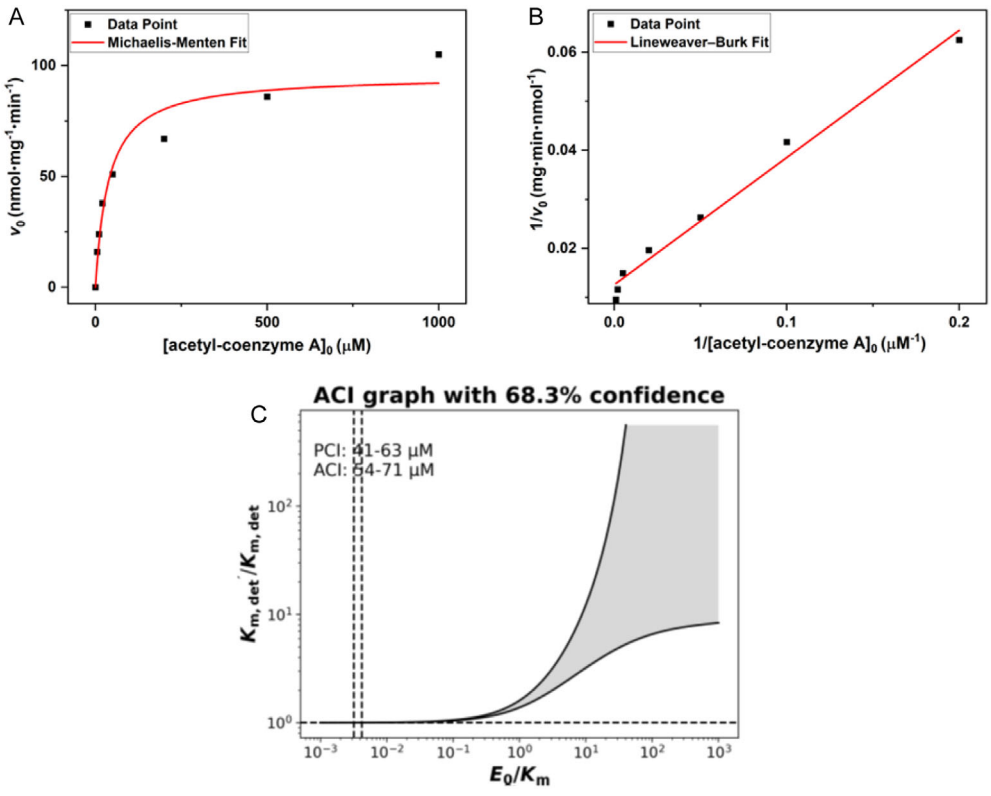

Figure 5. Application of ACI-Km to a retrospective K_m-determination dataset for the anaAT–acetyl-coenzyme a pair. A) Experimental MM plot "v_0 versus [pyruvate]$_0$" fitted using the MM model. B) Lineweaver–Burk transformation of the pseudosteady–state curve "$1/v_0$ versus 1/[pyruvate]$_0$" fitted with the linear Lineweaver–Burk model. C) ACI graph (68.3% confidence) generated by ACI-Km, from which the PCI of K_m was determined as 41–63 μM, and the ACI of K_m as 54–71 μM. (Panels **A** and **B** are adapted from Figure 6D in ref. [54]).

errors, the standard deviation for the CI of $|\Delta E_0/E_0|$ is unlikely to be below 10%.[56]

Since substrate concentrations typically span a higher range, from micromolar to millimolar levels, the associated inaccuracies from mass weighing, sample adsorption, serial dilution, and related sources are generally expected to be lower than those encountered in enzyme solution preparation. Nevertheless, due to inherent systematic uncertainties in mass and volume measurements during sample preparation, reducing the standard deviation for the CI of $|\Delta S_0/S_0|$ to below 5% remains challenging.[57] Therefore, in this study, we assigned relative standard deviations of 10% and 5% to the CIs of $|\Delta E_0/E_0|$ and $|\Delta S_0/S_0|$, respectively, for calculating the narrower limit of the ACI of K_m. The same values were subsequently applied in the analysis of the other experimental datasets.

By inputting the published dataset, the nominal enzyme concentration of 0.23 μM, and the proposed relative standard deviations for $|\Delta E_0/E_0|$ and $|\Delta S_0/S_0|$ (10% and 5%, respectively) into the ACI-Km webapp, the ACI and PCI for K_m were computed based on the numerically established ACI graph (i.e., Figure 5C). At a 68.3% confidence level, the ACI and PCI for K_m were determined to be 54–71 and 41–63 μM, respectively. Both intervals have similar widths and show substantial overlap, but the ACI provides a more statistical significance. The ACI estimate indicates that the accurate K_m value for AnaAT–acetyl-coenzyme A falls within the range of 54–71 μM with 68.3% confidence, which is substantially lower than the originally reported 96 μM, which was determined using the linearized MM model, specifically the Lineweaver–Burk plot.

In our previous study, we numerically demonstrated that employing a simplified fitting model, such as the K_d fitting model (mathematically analogous to the conventional MM equation) incorrectly assuming the ligand concentration to be negligible in K_d determination, can result in an overestimation of the K_d value.[23] The present experimental results for K_m determination further support this concept, confirming that a similar bias arises when using a simplified model, specifically the conventional MM equation, for K_m determination. This finding underscores the value of integrating K_d and K_m studies, for instance, by employing a unified binding-isotherm model for both K_d and K_m determinations, to facilitate cross-applicability and methodological consistency between these areas.

To further explore the application of the ACI concept in K_m determination, we conducted an experiment using lactate dehydrogenase (LDH) and pyruvate as the enzyme–substrate pair, with NADH as a co-substrate. In this experiment, the conversion of NADH to NAD^+ was monitored by measuring the decrease in absorbance at 340 nm, reflecting the rate of product formation. In this experiment, a nominal enzyme concentration of $[LDH]_0 = 0.87$ nM was used. The progress curves "P versus time" were recorded at initial pyruvate concentrations ($[pyruvate]_0$), from 23 to 2000 μM in 1.5-fold increments. From the recorded progress curves, we determined v_0 for product formation at each pyruvate concentration, which resulted in the MM plot "v_0 versus $[pyruvate]_0$" (**Figure 6**A). More experimental details are provided in Note S6, including Figure S4, Supporting Information. For comparison purposes, the fitting line to the MM plot using the MM equation is shown in Figure 6A, yielding a determined $K_{m,det}$ of 68 ± 4 μM (PCI: 64–72 μM) and a $v_{0,max}$ of $(12.4 \pm 0.2) \times 10^{-4}\,s^{-1}$. The agreement between the predicted $v_{0,max}$ and the measured v_0 ($(12.3 \pm 0.3) \times 10^{-4}\,s^{-1}$) at the highest initial pyruvate concentration ($[pyruvate]_0 = 2000$ μM) confirms the applicability of ACI–Km to this experimental MM plot.

The MM plot was analyzed using the ACI-Km program to compute the ACI and PCI of K_m for LDH–pyruvate. To determine the lower limit of the ACI for K_m, we assigned standard deviations of 10% and 5% to the CIs of $|\Delta E_0/E_0|$ and $|\Delta S_0/S_0|$, respectively, as previously described in the section on retrospective data. Although the lower bound of the CI for E_0/K_m fell below 0.001, the updated ACI-Km webapp successfully estimated the ACI of K_m as 62–70 μM, which was slightly wider than the PCI of 63–69 μM, both at 68.3% confidence (Figure 6B). Notably, at such an extremely low E_0/K_m ratio, when $v_{0,max}$ is experimentally measured, the PCI ranges determined by both the MM model and the binding-isotherm model closely agree, as theoretically expected. It is important to emphasize that, for the purpose of demonstrating the ACI-Km application, this ACI represents only its lower bound. This assumes negligible systematic uncertainty in the measured signals ($\Delta R/R$) and the absence of significant "true"

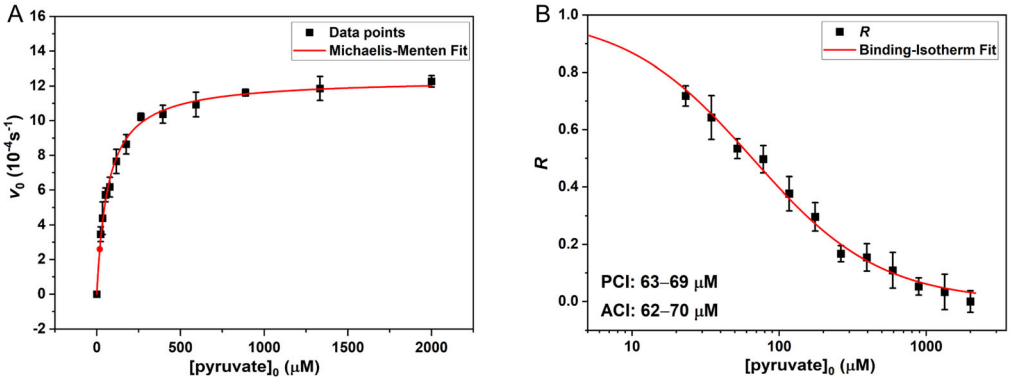

Figure 6. Application of the binding-isotherm model and ACI-Km to a K_m-determination experiment using LDH–pyruvate as the enzyme–substrate pair. A) Experimental MM plot "v_0 versus $[pyruvate]_0$" with an MM fit. B) Transformation of the MM plot into the binding-isotherm plots, fitted using the binding-isotherm model ((Equation 8)) to compute the PCI and ACI of K_m under conditions where the E_0/K_m ratio is lower than 0.001.

systematic errors in reagent concentrations or measured signals resulting from improper experimental practices.

3. Discussion

3.1. Comparative Considerations for ACI-Km and ACI-Kd

A key distinction between ACI-Km and ACI-Kd lies in their theoretical foundations. ACI-Km is rooted in the MM framework and therefore inherits the assumptions of the QSSA. By contrast, ACI-Kd is free of such constraints, as equilibrium dissociation constants are derived from binding isotherms that depend solely on the reversible equilibrium between ligand and target, without invoking QSSA. As a result, ACI-Kd quantifies systematic uncertainties without additional assumptions, whereas ACI-Km does not. This distinction explains why a broadened ACI produced by ACI-Km may serve only as a qualitative diagnostic warning sign when QSSA validity is in doubt, while ACI-Kd remains robust across the full range of binding experiments.

Unlike K_d determination, where the experimentally used ligand concentration is sometimes significantly higher than the true K_d due to the instrument's high LOQ values,[18,24] achieving $E_0/K_m < 1$ is generally more feasible, as commonly studied K_m values (within the micromolar range) are usually much larger than typical K_d values (in the picomolar to nanomolar range). Nevertheless, calculating the ACI of K_m remains crucial, as our study indicated that obtaining an accurate K_m depends on satisfying the condition $E_0/K_m < a/b$ (Figure 2B) rather than $E_0/K_m < 1$. Since the parameters a and b are defined by the relative systematic errors of the variables (Note S2, Supporting Information), the ratio a/b can be significantly less than unity if the variables are subject to large systematic errors, which is possible in K_m determination.[24,58,59] Consequently, a wide ACI may still be obtained even when $E_0/K_m < 1$. In such cases, experimentalists may need to further reduce E_0 to achieve a narrower ACI for K_m that aligns with the accuracy required for their specific enzymatic application.

Finally, similar to ACI-Kd, the reliability of K_m values derived from ACI-Km depends on practical assumptions, including minimized systematic errors in reagent preparation and the validity of the regression model. While these assumptions are typically met in well-controlled experiments, even when they are not fully satisfied, the ACI framework still produces a robust lower-bound estimate of systematic uncertainty. This ensures that ACI remains a valuable diagnostic tool for assessing the minimal confidence limits of K_m under realistic experimental conditions.

3.2. Limitations of ACI-Km

The applicability of ACI-Km, like that of the MM equation itself, is bounded by the assumptions of the QSSA on which the MM model is based. The framework quantifies accuracy within this mathematical regime, which assumes that enzyme concentration is much lower than the combined substrate and Michaelis constant ($E_0 << S_0 + K_m$) and that the enzyme–substrate complex forms rapidly relative to turnover ($k_{-1} + k_2 >> k_1(E_0 + S_0)$). These conditions need not be verified a priori, but significant deviation from them manifests as broader ACI intervals, reflecting reduced numerical identifiability of K_m within the MM model. In this sense, ACI-Km not only quantifies accuracy but also serves as a diagnostic indicator of possible violations of the steady-state assumption.[32,60,61]

ACI-Km does not correct systematic errors in the experimental variables. It quantifies how residual systematic uncertainties in concentrations propagate, and may be amplified, into the determined K_m values. In its present form, the framework treats concentration-related sources, primarily $\Delta E_0/E_0$ and $\Delta S_0/S_0$, and only to a limited extent $\Delta R/R$ when a credible confidence interval for the experimental signals can be specified. Other systematic biases, such as instrument calibration drift, baseline instability, temperature variation, pipetting inaccuracy, and detector nonlinearity, lie outside the quantitative scope of ACI-Km. These must be minimized by calibration and rigorous protocols before applying the analysis, so that the intervals reported by ACI-Km reflect residual concentration-related uncertainties rather than avoidable experimental artifacts.

Passing the ACI test does not prove that the result is correct. A narrow ACI only indicates that, under the assumed model and the user-supplied CIs for concentration errors, the propagation to $K_{m,det}$ is limited. It does not exclude unmodeled sources of bias, model misspecification, or violations of the QSSA. In this sense, ACI-Km functions as a test for badness rather than a test for goodness. A wide ACI is an actionable warning of potential inaccuracy or model breakdown, whereas a narrow ACI indicates only the absence of such diagnostic warnings and should be interpreted together with independent checks of assumptions and experimental controls.

The same diagnostic logic applies to precision metrics. A narrow PCI or SE reflects low random variability under the chosen model but does not guarantee reproducibility or freedom from unmodeled random uncertainties. Likewise, a narrow ACI does not confirm the correctness of $K_{m,det}$, only that the propagation of the specified systematic uncertainties is limited. Both ACI and PCI should therefore be interpreted as tests for badness rather than proofs of goodness, serving complementary roles in identifying potential weaknesses in experimental design and data reliability.

Despite this inherent diagnostic value, ACI-Km still has several limitations that we plan to address in future work. First, applying the binding-isotherm model (Equation 8) requires that the saturation condition ($S_0 >> K_m$) be achieved at the highest substrate concentration to directly estimate $v_{0,max}$. In practice, this condition should be verified experimentally by confirming that the reaction rate approaches a plateau at the highest substrate concentration, indicating that $v_{0,max}$ has been reached or closely approximated. In some assays, this may be infeasible due to substrate solubility limits. Although one might consider using a fitting model that estimates K_m and $v_{0,max}$ simultaneously, increasing the number of fitted parameters typically compromises the accuracy of the key parameter of interest,[25,26] K_m in this case. Second, ACI-Km currently neglects systematic

uncertainties in R values, since typically only random errors are accessible, owing to the lack of a reliable method for their determination. Establishing a systematic approach to quantify and incorporate these uncertainties into ACI calculations will be an important goal for future work. It should also be emphasized that applying ACI-Km requires prior elimination of genuine systematic errors in concentrations and signals, such as those arising from improper instrument calibration, baseline drift, or reagent impurities, through optimized experimental protocols or mathematical corrections. The systematic uncertainties considered in ACI-Km should therefore reflect only the unavoidable residual systematic errors that cannot be fully eliminated. Third, although accounting for systematic uncertainties in experimental variables broadens the uncertainty range of the determined K_m, it does not directly resolve ranking errors that arise when catalytic efficiencies (k_2/K_m) are compared using values derived from single-point K_m estimates (e.g., Figure 1A). Broader ACIs can make enzyme rankings indistinguishable through overlap; critically, such overlap signals the need to improve experimental conditions (e.g., lowering E_0) and the accuracy of concentration and signal measurements before drawing conclusions. Such precautions are crucial to avoid costly misinterpretations in both academic studies and industrial applications.

4. Conclusions

In this work, we established the mathematical parallels between K_m and K_d determinations, showing that both can be described by a unified binding-isotherm model (Equation 8). This framework, which requires a reliable determination of $v_{0,max}$ under substrate saturation, enables methodologies developed for K_d accuracy to be applied directly to K_m. Building on this, we reiterated the ACI workflow (Figure 3), verified its use for K_m (Figure 4), and incorporated ACI-Km functionality into the ACI webapp (https://aci.sci.yorku.ca), extending applicability across the full E_0/K_m range. The webapp was validated with synthetic data and demonstrated in real K_m-determination experiments. Retrospective analysis of published datasets revealed that conventional MM or Lineweaver–Burk analysis can overestimate K_m even when $E_0 << S_0 + K_m$ is satisfied. Finally, we introduced a strategy for computing ACI of K_m under the condition of $E_0/K_m \leq 0.01$, where $K_{m,det}$ is insensitive to E_0, and successfully applied it to the LDH–pyruvate system.

Despite its benefits, ACI-Km still faces several limitations, including the difficulty of achieving substrate saturation at high S_0, the lack of a systematic method to incorporate systematic uncertainties in R values, and unresolved ranking errors in catalytic efficiency (k_2/K_m) when based on single-point K_m estimates. While ACI-Km represents a significant step toward quantitative accuracy assessment in enzyme kinetics, it remains an evolving diagnostic framework. Its current form quantifies only concentration-related systematic uncertainties and should be interpreted as a diagnostic aid for identifying and mitigating potential inaccuracies (e.g., from stock solution errors or QSSA violations), rather than as a universal solution. Addressing these issues will be an important direction for future work. With its advances, ACI-Km, when combined with PCI assessment, has the potential to become a powerful framework for more accurate and reliable enzyme kinetics. Beyond reducing misinterpretations in fundamental research, this approach may also provide useful guidance for enzyme engineering, inhibitor screening, and metabolic modeling in academic settings and offer practical value for improving reliability in bioprocess optimization and drug development.

5. Experimental Section

Materials and Solutions

Both the NADH disodium salt and pyruvate acid sodium salt were purchased from Carl Roth GmbH + Co. KG (Karlsruhe, Germany). The lactate dehydrogenase (LDH) from rabbit muscle was purchased from Merck KGaA (Darmstadt, Germany). PBS buffer was obtained from Carl Roth GmbH + Co. KG (Karlsruhe, Germany). All solutions were prepared in the PBS buffer.

Kinetic Assays

The kinetic assays were performed in flat-bottom 96-well plates (Greiner Bio-One GmbH, Frickenhausen, Germany) using a microplate plate reader (Tecan Infinite M200Pro, Tecan, Männedorf, Switzerland). All measurements were performed in a final volume of 200 µL at 23 °C. The experiment was performed with an LDH concentration of 0.87 nM. The concentration of NADH was kept constant at 500 µM in all experiments. The pyruvate concentration was varied from the lowest nonzero concentration of 23 to 2000 µM in 1.5-fold increments, resulting in 13 data points, including one at 0 µM. After the addition of pyruvate, the 96-well plate was immediately placed in the microplate reader, and the formation of NAD^+ was measured at 340 nm every 10 s for a total of 490 s. The values of v_0 were determined from the change in NAD^+ concentration within the first 250 s and used to generate MM plots ("v_0 vs $[pyruvate]_0$"). All measurements were performed in triplicate.

Acknowledgements

This work was supported by a York University grant to the Catalyzing Interdisciplinary Research Cluster "Technologies for Identification and Control of Infectious Diseases" and an NSERC Discovery grant number RGPIN-2022−04563 to SNK. The authors acknowledge the use of ChatGPT (OpenAI) to improve the clarity and readability of the manuscript. The AI tool was employed for language refinement, grammar correction, and overall enhancement of writing style, while all scientific content, interpretations, and conclusions were solely determined by the authors.

Conflict of Interest

The authors declare no conflict of interest.

Data Availability Statement

The data that support the findings of this study are openly available in [Figshare] at [https://doi.org/10.6084/m9.figshare.26961733], reference number [26961733].

Keywords: accuracy confidence interval · error propagation · Michaelis constant · precision confidence interval · regression stability test

[1] L. Michaelis, M. L. Menten, *Biochem. Z.* **1913**, *49*, 352.
[2] G. E. Briggs, J. B. S. Haldane, *Biochem. J.* **1925**, *19*, 338.
[3] L. A. Segel, M. Slemrod, *SIAM Rev.* **1989**, *31*, 446.
[4] J. Chapman, A. E. Ismail, C. Z. Dinu, *Catalysts* **2018**, *8*, 238.
[5] M. Kalp, A. Sheri, J. D. Buynak, C. R. Bethel, R. A. Bonomo, P. R. Carey, *J. Biol. Chem.* **2007**, *282*, 21588.
[6] A. Badarau, Q. Shi, J. W. Chow, J. Zajicek, S. Mobashery, S. Vakulenko, *J. Biol. Chem.* **2008**, *283*, 7638.
[7] N. A. Simeth, T. Kinateder, C. Rajendran, J. Nazet, R. Merkl, R. Sterner, B. König, A. C. Kneuttinger, *Chem. Eur. J.* **2021**, *27*, 2439.
[8] N. Balachandran, M. Heimhalt, P. Liuni, F. To, D. J. Wilson, M. S. Junop, P. J. Berti, *Biochemistry* **2016**, *55*, 6617.
[9] R. Panchagnula, N. S. Thomas, *Int. J. Pharm.* **2000**, *201*, 131.
[10] P. Mendes, D. Kell, *Bioinformatics* **1998**, *14*, 869.
[11] R. Govind, C. Gao, L. Laai, X. Yan, S. Pfanstiel, H. Tabak, *Appl. Biotechnol. Site Rem.* **1994**, *2*, 229.
[12] M. Chandrasekaran, *Enzymes in Food and Beverage Processing*, CRC Press, Boca Raton, FL, USA **2016**.
[13] E. Csöoregi, S. Gáspñr, M. Niculescu, B. Mattiasson, W. Schuhmann, *Physics and Chemistry Basis of Biotechnology*, Springer, Dordrecht **2002**, pp. 105–129.
[14] J. C. Goldsack, A. Coravos, J. P. Bakker, B. Bent, A. V. Dowling, C. Fitzer-Attas, A. Godfrey, J. G. Godino, N. Gujar, E. Izmailova, C. Manta, B. Peterson, B. Vandendriessche, W. A. Wood, K. W. Wang, J. Dunn, *Npj Digit. Med.* **2020**, *3*, 55.
[15] G. Atkins, I. Nimmo, *Anal. Biochem.* **1980**, *104*, 1.
[16] G. Sagnella, *Trends Biochem. Sci.* **1985**, *10*, 100.
[17] C. M. Hill, R. D. Waightm, W. G. Bardsley, *Mol. Cell Biochem.* **1977**, *15*, 173.
[18] T. Y. Wang, J. Latimer, J. L. Rukundo, I. Kogan, S. M. Krylova, S. Schreiber, P. Kohlmann, J. Jose, S. N. Krylov, *Precis. Chem.* **2025**, *3*, 89.
[19] Y.-S. Cho, H.-S. Lim, *Transl. Clin. Pharmacol.* **2018**, *26*, 39.
[20] P. C. Buchholz, R. Ohs, A. C. Spiess, J. Pleiss, *Biotechnol. J.* **2019**, *14*, 1800183.
[21] S. Schnell, *FEBS J.* **2014**, *281*, 464.
[22] J. Bentz, T. T. Tran, J. W. Polli, A. Ayrton, H. Ellens, *Pharm. Res.* **2005**, *22*, 1667.
[23] T. Y. Wang, J.-L. Rukundo, Z. Mao, S. N. Krylov, *ACS Chem. Biol.* **2024**, *19*, 1852.
[24] T. Y. Wang, H. Ji, D. Everton, A. T. Le, S. M. Krylova, R. Fournier, S. N. Krylov, *Anal. Chem.* **2023**, *95*, 15826.
[25] M. Davidian, D. M. Giltinan, *J. Agric. Biol. Environ. Stat.* **2003**, *8*, 387.
[26] D. G. Kleinbaum, L. L. Kupper, K. E. Muller, A. Nizam, *Applied Regression Analysis and Other Multivariable Methods*. Vol. *601*, Duxbury Press, Belmont, CA **1988**.
[27] B. M. Zhao, S. L. Keasey, J. E. Tropea, G. T. Lountos, B. K. Dyas, S. Cherry, S. Raran-Kurussi, D. S. Waugh, R. G. Ulrich, *PloS One* **2015**, *10*, e0134984.
[28] I. I. Udema, *WJARR* **2022**, *16*, 350.
[29] J. R. Mathis, K. Back, C. Starks, J. Noel, C. D. Poulter, J. Chappell, *Biochemistry* **1997**, *36*, 8340.
[30] A. R. Tzafriri, *Bull. Math. Biol.* **2003**, *65*, 1111.
[31] S. Cha, *J. Biol. Chem.* **1970**, *245*, 4814.
[32] S. Schnell, P. K. Maini, *Bull. Math. Biol.* **2000**, *62*, 483.
[33] B. Choi, G. A. Rempala, J. K. Kim, *Sci. Rep.* **2017**, *7*, 17018.
[34] M. Kanoatov, V. A. Galievsky, S. M. Krylova, L. T. Cherney, H. K. Jankowski, S. N. Krylov, *Anal. Chem.* **2015**, *87*, 3099.
[35] T. Little, *BioPharm Int.* **2015**, *28*. 48.
[36] I. Pérez, *Eur. J. Phys.* **2011**, *32*, 993.
[37] G. Guercio, V. Zanetti, *Am. J. Phys.* **1987**, *55*, 59.
[38] W. D. van Marken Lichtenbelt, H. A. Daanen, L. Wouters, R. Fronczek, R. J. Raymann, N. M. Severens, E. J. Van Someren, *Physiol. Behav.* **2006**, *88*, 489.
[39] G. Bolt, *J. Phys. Chem.* **1957**, *61*, 1166.
[40] T.-S. Chen, *IEEE Trans. Microw. Theory Tech.* **1960**, *8*, 510.
[41] R. O'brien, D. Cannon, W. Rowlands, *J. Colloid Interface Sci.* **1995**, *173*, 406.
[42] P. D. Domich, J. Baker-Jarvis, R. G. Geyer, *J. Res. Natl. Inst. Stand. Technol.* **1991**, *96*, 565.
[43] B. Pathare, V. Tambe, V. Patil, *Int. J. Pharm. Pharm. Sci.* **2014**, *6*, 26.
[44] P. Janoš, *J. Chromatogr. A.* **2004**, *1037*, 15.
[45] D. J. Currie, *Biometrics* **1982**, *38*, 907.
[46] J. Matthews, G. Allcock, *Stat. Med.* **2004**, *23*, 477.
[47] K.-I. Yun, T.-S. Han, *Biochimie* **2020**, *176*, 12.
[48] N. P. Kazmierczak, J. A. Chew, D. A. V. Griend, *Anal. Chim. Acta.* **2022**, *1227*, 339834.
[49] T. H. Nguyen, A. S. Rustenburg, S. G. Krimmer, H. Zhang, J. D. Clark, P. A. Novick, K. Branson, V. S. Pande, J. D. Chodera, D. D. Minh, *PLoS One* **2018**, *13*, e0203224.
[50] F. Feng, T. B. Kepler, *PloS One* **2015**, *10*, e0130812.
[51] A. S. Avaro, J. G. Santiago, *Angew. Chem., Int. Ed.* **2022**, *134*, e202209527.
[52] L. A. Segel, *Bull. Math. Biol.* **1988**, *50*, 579.
[53] H. Bisswanger, *Sci. Perspect.* **2014**, *1*, 41.
[54] W.-B. Yin, A. Grundmann, J. Cheng, S.-M. Li, *J. Biol. Chem.* **2009**, *284*, 100.
[55] J. V. Passonneau, O. H. Lowry, *Enzymatic Analysis: A Practical Guide*, Springer Science & Business Media, NY **2008**.
[56] T. Tiffany, P. Thayer, C. Coelho, G. Manning, *Clin. Chem.* **1976**, *22*, 1438.
[57] J. A. Lyn, M. H. Ramsey, R. J. Fussell, R. Wood, *Analyst* **2003**, *128*, 1391.
[58] S. Schnell, S. M. Hanson, *Biophys. Chem.* **2007**, *125*, 269.
[59] N. J. Kruger, *Phytochemistry* **1995**, *38*, 1065.
[60] G. E. Briggs, J. B. Haldane, *Biochem. J.* **1925**, *19*, 338.
[61] I. H. Segel, *Enzyme Kinetics: Behavior and Analysis of Rapid Equilibrium and Steady State Enzyme Systems*. Vol. *115*, Wiley, New York **1975**.

Manuscript received: August 29, 2025
Revised manuscript received: October 24, 2025
Version of record online: November 18, 2025

SUPPORTING INFORMATION

Introducing Quantitative Assessment of Michaelis Constant (K_m) Accuracy

Tong Ye Wang,[a, b] Parmeetpal Dhillon,[a, b] Svetlana M. Krylova,[a, b] Amit Bijlani,[a, b] Sebastian Schreiber,[c] Dasantila Golemi-Kotra,[b, d] Joachim Jose,[c] and Sergey N. Krylov*[a, b]

[a] Department of Chemistry, York University, 4700 Keele St, Toronto, ON M3J 1P3, Canada

[b] Centre for Research on Biomolecular Interactions, York University, 4700 Keele St, Toronto, ON M3J 1P3, Canada

[c] Institute of Pharmaceutical and Medicinal Chemistry, University of Münster, Münster, Germany 48149

[d] Department of Biology, York University, 4700 Keele St, Toronto, ON M3J 1P3, Canada

*Corresponding author's email address: skrylov@yorku.ca

Table of Contents

Additional supplementary files

The following supplementary files can be found on Figshare:
https://doi.org/10.6084/m9.figshare.26961733

File name	Description/Experiment
Figures.zip	Figures in main text and supporting information (Origin and png files).
Synthetic_data.xlsx	Spreadsheet for simulated reaction progress curves (Excel file).
Experimental_data.xlsx	Raw data and preliminary data analysis for experiments (Excel file).
rankingKmSim.txt	Script of the "rankingKmSim" program (txt file).

Note S1: Simulated enzyme ranking experiment and comparison between the true ranks and the determined ranks

To simulate a simple enzyme–substrate ranking experiment, we developed a Python script (rankingKmSim.py, available at https://doi.org/10.6084/m9.figshare.26961733) that generates synthetic progress curves and analyzes them using conventional data-analysis procedures. Specifically, the script: (*i*) simulates progress curves of product concentration (P) versus time (t) by numerically solving the system of ordinary differential equations that describe the reaction mechanism outlined in eq S1,

$$\begin{aligned} \frac{dS}{dt} &= -k_1 ES + k_{-1} C \\ \frac{dC}{dt} &= k_1 ES - (k_{-1} + k_2) C \\ \frac{dP}{dt} &= k_2 C \end{aligned} \tag{S1}$$

based on user-specified parameters including the kinetic rate constants k_1, k_{-1}, and k_2, as well as the initial enzyme concentration (E_0) and initial substrate concentration (S_0); (*ii*) calculates the initial reaction velocity (v_0) for each S_0 at a fixed E_0, based on the slope of the simulated progress curve; (*iii*) constructs a Michaelis–Menten (MM) plot of v_0 versus S_0; and (*iv*) fits the MM plot to the classical MM equation (eq S2),

$$v_0 = \frac{v_{0,\max} S_0}{K_\mathrm{m} + S_0} \tag{S2}$$

using a least-squares approach to determine the apparent Michaelis constant ($K_{\mathrm{m,det}}$) and estimate the maximum initial reaction velocity ($v_{\mathrm{o,max}}$).

The experiment included 10 enzyme–substrate pairs, labeled "pair 01" through "pair 10," each assigned known kinetic parameters with input (true) K_m values ranging from 50 to 230 μM in 20 μM increments. For all pairs, k_2 = 10 $\mu M^{-1}s^{-1}$, k_{-1} = 100 s^{-1}, and E_0 = 10 μM. For each pair, ten substrate concentrations were chosen to span a logarithmic range from 0.1K_m to 10K_m, ensuring appropriate sampling across the MM curve.

To reflect realistic experimental conditions, systematic errors were introduced: relative errors of $\Delta E_0/E_0$ = 0.2 and $\Delta S_0/S_0$ = 0.2 were applied to enzyme and substrate concentrations, respectively. Additionally, Gaussian noise (2% of signal) was added to the simulated progress curves. Each enzyme thus had 10 progress curves, each corresponding to a different S_0, spanning an 80-second time window sampled at 1-second intervals.

Initial reaction velocities (v_0) were extracted by fitting a straight line to the early, linear portion of each progress curve, defined as the region preceding 10% substrate depletion. Linearity of these fits was confirmed visually. The resulting S_0 versus v_0 data were analyzed using the standard MM equation (eq S2) via unweighted least-squares regression in Python (equivalent to use the commercial data-analysis software, e.g., GraphPad Prism and Origin) to obtain estimates of K_m and $v_{0,\max}$, along with their standard errors. k_2 was then computed from the estimated $v_{0,\max}$ and known E_o (with systematic error) using eq S3:

$$k_2 = \frac{v_{0,\max}}{E_0} \tag{S3}$$

Catalytic efficiencies (k_2/K_m) were then calculated, and the enzyme–substrate pairs were ranked based on the calculated catalytic efficiencies and compared to rankings based on the true input parameters.

The script also computed the relative systematic error in determined K_m ($|\Delta K_m/K_m|$) and plotted it against the true value of E_0/K_m (Figure 1B in the main text). All simulation parameters, numerical settings, and fitting procedures are fully documented in rankingKmSim.py. Final ranking results are presented in Table S1, where a rank of #1 corresponds to the highest catalytic efficiency.

As shown in Table S1, when experimental variables, such as reactant concentrations, are subject to realistic systematic errors, and when the MM plots do not extend sufficiently into the saturation region (i.e., the plateau), classic K_m-determination experiments become vulnerable to enzyme mis-ranking. Such mis-ranking can lead to significant misinterpretation of catalytic performance, potentially compromising downstream decisions in enzyme selection and optimization.

Table S1. True versus determined catalytic-efficiency rankings.

Rank Number (#1 = Highest)	True Ranking	Determined Ranking
#1	pair_01	pair_04
#2	pair_02	pair_03
#3	pair_03	pair_06
#4	pair_04	pair_05
#5	pair_05	pair_02
#6	pair_06	pair_08
#7	pair_07	pair_07
#8	pair_08	pair_09
#9	pair_09	pair_01
#10	pair_10	pair_10

Note S2: Dependencies of the coefficients on the relative systematic errors of variables

The detailed dependencies of coefficients a and b, as well as α, λ, and β on $|\Delta T_0/T_0|$, $|\Delta L_0/L_0|$, and $|\Delta R/R|$ were presented in our previous work on K_d determination.[1] In this study, due to the mathematical similarity between K_d and K_m determinations, we can extend these results by replacing $|\Delta T_0/T_0|$ and $|\Delta L_0/L_0|$ with $|\Delta S_0/S_0|$ and $|\Delta E_0/E_0|$, respectively. This substitution allows us to derive the dependencies of a, b, α, λ, and β on $|\Delta S_0/S_0|$, $|\Delta E_0/E_0|$, and $|\Delta R/R|$.

By defining the relative systematic errors in S_0, E_0, and R as $|\Delta S_0/S_0| = s$, $|\Delta E_0/E_0| = e$, and $|\Delta R/R| = r$, the following dependencies can be obtained:

$$a = s + \frac{r(1+r)}{0.5+r},\ b = \frac{0.5(s+e-r)}{1+r} + \frac{0.5r}{0.5+r} \text{ when } 0 \le \Delta R < 0.5$$

$$a = s + \frac{r(1-r)}{0.5-r},\ b = \frac{0.5(s+e-r)}{1-r} + \frac{0.5r}{0.5-r} \text{ when } -0.5 < \Delta R < 0$$

$$\alpha = \sqrt{s^2 + \left(\frac{r(1+r)}{0.5}\right)^2},\ \beta = \frac{0.5}{1+r}\sqrt{s^2+e^2+r^2},\ \lambda = \frac{s^2}{1+r} + 2r^2 \text{ when } 0 \le \Delta R < 0.5 \quad \text{(S4)}$$

$$\alpha = \sqrt{s^2 + \left(\frac{r(1-r)}{0.5}\right)^2},\ \beta = \frac{0.5}{1-r}\sqrt{s^2+e^2+r^2},\ \lambda = \frac{s^2}{1-r} + 2r^2 \text{ when } -0.5 < \Delta R < 0$$

Note S3: Determination of the relative systematic errors in concentrations that define the ACI of K_m with different confidence levels

Eq 6 in the main text shows that:

$$K_m = \frac{S_0 - E_0(1-R)}{(1/R-1)} \quad \text{(S5)}$$

When the error sources of S_0, E_0, and R are fully correlated, the maximum systematic error of K_m can be calculated with the error propagation rule:[1-2]

$$|\Delta K_m| = \left|\left(\frac{\partial K_m}{\partial S_0}\right)\Delta S_0\right| + \left|\left(\frac{\partial K_m}{\partial E_0}\right)\Delta E_0\right| + \left|\left(\frac{\partial K_m}{\partial R}\right)\Delta R\right| \quad \text{(S6)}$$

However, when calculating the systematic error in K_m propagated from the specific systematic errors of variables, which may have different signs and result in ΔK_m with varying signs, it is important to use the formula without applying absolute values:[1, 3]

$$\Delta K_m = \left(\frac{\partial K_m}{\partial S_0}\right)\Delta S_0 + \left(\frac{\partial K_m}{\partial E_0}\right)\Delta E_0 + \left(\frac{\partial K_m}{\partial R}\right)\Delta R \quad \text{(S7)}$$

Note that, for uncorrelated error sources of S_0, E_0, and R, we can also use eq S7 to find the relative systematic errors in variables that define the ACI of K_m at various confidence levels.

Applying the error propagation rule eq S7 to eq S5 yields the following result:

$$\Delta K_m = \frac{R}{1-R}\Delta S_0 - R\Delta E_0 + \left(-E_0 + \frac{S_0}{(1-R)^2}\right)\Delta R \quad \text{(S8)}$$

By solving eq S5 for S_0, we obtain:

$$S_0 = (1/R-1)K_m + (1-R)E_0 \quad \text{(S9)}$$

To derive a closed-form solution for error propagation in eq S8, it is essential to focus on a single data point by fixing R. In this case, we focus on the scenario where the determined value of R is 0.5 with a systematic error ΔR, which approximates the least erroneous case.[1-2, 4] The actual value of R is then given by:

$$R = 0.5 - \Delta R \tag{S10}$$

and accordingly, eq S9 is converted to:

$$S_0 = \frac{(0.5 + \Delta R) K_\mathrm{m}}{0.5 - \Delta R} + (0.5 + \Delta R) E_0 \tag{S11}$$

Dividing both sides of eq S8 by K_m yields:

$$\frac{\Delta K_\mathrm{m}}{K_\mathrm{m}} = \frac{R}{1-R}\frac{\Delta S_0}{K_\mathrm{m}} - R\frac{\Delta E_0}{K_\mathrm{m}} + \left(-\frac{E_0}{K_\mathrm{m}} + \frac{1}{(1-R)^2}\frac{S_0}{K_\mathrm{m}} \right)\Delta R \tag{S12}$$

which can be rewritten as:

$$\frac{\Delta K_\mathrm{m}}{K_\mathrm{m}} = \frac{R}{1-R}\left(\frac{\Delta S_0}{S_0} \right)\frac{S_0}{K_\mathrm{m}} - R\frac{\Delta E_0}{E_0}\frac{E_0}{K_\mathrm{m}} + \left(-\frac{E_0}{K_\mathrm{m}} + \frac{1}{(1-R)^2}\frac{S_0}{K_\mathrm{m}} \right)\Delta R \tag{S13}$$

By inserting eqs S10 and S11 into eq S13, we obtain:

$$\begin{aligned} \frac{\Delta K_\mathrm{m}}{K_\mathrm{m}} = {} & \frac{0.5 - \Delta R}{0.5 + \Delta R}\left(\frac{\Delta S_0}{S_0} \right)\left[\frac{0.5 + \Delta R}{0.5 - \Delta R} + \frac{E_0}{K_\mathrm{m}}(0.5 + \Delta R) \right] - (0.5 - \Delta R)\frac{\Delta E_0}{E_0}\frac{E_0}{K_\mathrm{m}} \\ & + \left[-\frac{E_0}{K_\mathrm{m}} + \frac{1}{(0.5 + R)^2}\left(\frac{0.5 + \Delta R}{0.5 - \Delta R} + \frac{E_0}{K_\mathrm{m}}(0.5 + \Delta R) \right) \right]\Delta R \end{aligned} \tag{S14}$$

To express ΔR through the relative systematic error of R (i.e., $\Delta R/R$), we have:

$$\begin{aligned} & \Delta R = R\frac{\Delta R}{R} = (0.5 - \Delta R)\frac{\Delta R}{R} \Rightarrow \Delta R = 0.5\frac{\Delta R}{R} - \Delta R\frac{\Delta R}{R} \Rightarrow \left(1 + \frac{\Delta R}{R} \right)\Delta R = 0.5\frac{\Delta R}{R} \\ & \Rightarrow \Delta R = \frac{0.5\dfrac{\Delta R}{R}}{1 + \dfrac{\Delta R}{R}} \end{aligned} \tag{S15}$$

Finally, substituting eq S15 into eq S14 gives:

$$\frac{\Delta K_m}{K_m} = \frac{0.5\Delta S_0/S_0}{0.5+\Delta R/R}\left[\frac{0.5+\Delta R/R}{0.5}+\frac{0.5+\Delta R/R}{1+\Delta R/R}\frac{E_0}{K_m}\right]-\frac{0.5\Delta E_0/E_0}{1+\Delta R/R}\frac{E_0}{K_m}$$
$$+\left[-\frac{E_0}{K_m}+\left(\frac{1+\Delta R/R}{0.5+\Delta R/R}\right)^2\left(\frac{0.5+\Delta R/R}{0.5}+\frac{0.5+\Delta R/R}{1+\Delta R/R}\frac{E_0}{K_m}\right)\right]\frac{0.5\Delta R/R}{1+\Delta R/R}$$
$$\Rightarrow \frac{\Delta K_m}{K_m} = \left[\frac{0.5\left(\Delta S_0/S_0-\Delta E_0/E_0-\Delta R/R\right)}{1+\Delta R/R}+\frac{0.5\Delta R/R}{0.5+\Delta R/R}\right]\frac{E_0}{K_m}$$
$$+\left[\Delta S_0/S_0+\frac{\Delta R/R\left(1+\Delta R/R\right)}{0.5+\Delta R/R}\right] \quad \text{(S16)}$$

If we define $K_{m,det}$ and K_m as the experimentally determined and true (unknown) K_m values, respectively, by incorporating the definition of the systematic error of K_m (i.e., $\Delta K_m = K_{m,det} - K_m$) into eq S16, we obtain:

$$\frac{K_{m,det}-K_m}{K_m} = \frac{K_{m,det}}{K_m}-1$$
$$=\left[\frac{0.5\left(\Delta S_0/S_0-\Delta E_0/E_0-\Delta R/R\right)}{1+\Delta R/R}+\frac{0.5\Delta R/R}{0.5+\Delta R/R}\right]\frac{E_0}{K_m}$$
$$+\left[\Delta S_0/S_0+\frac{\Delta R/R\left(1+\Delta R/R\right)}{0.5+\Delta R/R}\right]$$
$$\Rightarrow \frac{K_{m,det}}{K_m} = \left[\frac{0.5\left(\Delta S_0/S_0-\Delta E_0/E_0-\Delta R/R\right)}{1+\Delta R/R}+\frac{0.5\Delta R/R}{0.5+\Delta R/R}\right]\frac{E_0}{K_m}$$
$$+\left[\Delta S_0/S_0+\frac{\Delta R/R\left(1+\Delta R/R\right)}{0.5+\Delta R/R}+1\right] \quad \text{(S17)}$$

If the guidelines from our previous work for minimizing systematic concentration errors are strictly followed, we can reasonably assume that the confidence intervals for ΔS_0 and ΔE_0 are governed by normally-distributed random errors in the stock solution concentrations, denoted as δS_0 and δE_0.[2, 5] In contrast, at this point, we have not established a quantitative method for assessing the confidence interval of ΔR.[2, 5] Therefore, in the absence of input data for ΔR, we will focus solely on the systematic errors of S_0 and E_0, disregarding ΔR, to derive narrower confidence intervals for K_m at the specified confidence levels. Under these conditions, eq S17 simplifies as follows (with $\Delta R/R$ excluded):

$$\frac{K_{m,det}}{K_m} = 0.5\left(\frac{\Delta S_0}{S_0}-\frac{\Delta E_0}{E_0}\right)\frac{E_0}{K_m}+\frac{\Delta S_0}{S_0}+1 \quad \text{(S18)}$$

If we assume that the confidence levels for ΔE_0 and ΔS_0 are always identical, then to achieve a 68.3% confidence level for K_m, the confidence levels for both ΔE_0 and ΔS_0 should be equal to $(68.3\%)^{1/2}$, which is approximately 82.6%. To determine the number of standard deviations needed to cover 82.6% of the probability distribution for the concentrations of enzyme or substrate (centred around their nominal values), we consulted the positive standard normal (Z-score) table.[6] As a result, we selected the intervals $\Delta E_0/E_0 \in [-1.36\delta E_0/E_0,\ 1.36\delta E_0/E_0]$ and $\Delta S_0/S_0 \in [-1.36\delta S_0/S_0,\ 1.36\delta S_0/S_0]$ as the confidence intervals for the relative systematic errors of E_0 and S_0, respectively, to achieve a 68.3% confidence level for K_m.

Using the same approach, we determined that for a 95.5% confidence level of K_m, the confidence intervals for the relative systematic errors are $\Delta E_0/E_0 \in [-2.27\delta E_0/E_0,\ 2.27\delta E_0/E_0]$ and $\Delta S_0/S_0 \in [-2.27\delta S_0/S_0,\ 2.27\delta S_0/S_0]$. For a 99.7% confidence level, the intervals expand to $\Delta E_0/E_0 \in [-3.18\delta E_0/E_0,\ 3.18\delta E_0/E_0]$ and $\Delta S_0/S_0 \in [-3.18\delta S_0/S_0,\ 3.18\delta S_0/S_0]$.

Next, we need to determine the combinations of $\Delta E_0/E_0$, $\Delta S_0/S_0$ (and $\Delta R/R$) that correspond to the relative systematic errors in the variables, yielding the smallest and largest accuracy ratios, $K_{m,det}/K_m$. From eq S18, we can infer that the accuracy ratio $K_{m,det}/K_m$ is minimized when $\Delta E_0/E_0$ is at the upper bound of its confidence interval (i.e., $1.36\delta E_0/E_0$) and $\Delta S_0/S_0$ is at the lower bound (i.e., $-1.36\delta S_0/S_0$). Therefore, the vectors $\{\Delta E_0/E_0 = 1.36\delta E_0/E_0,\ \Delta S_0/S_0 = -1.36\delta S_0/S_0\}$ and $\{\Delta E_0/E_0 = -1.36\delta E_0/E_0,\ \Delta S_0/S_0 = 1.36\delta S_0/S_0\}$ will define the ACI for K_m at a 68.3% confidence level through the error propagation of nonlinear regression.

A similar approach can be applied to identify the values of $\Delta E_0/E_0$ and $\Delta S_0/S_0$ that define the ACI for K_m at higher confidence levels, such as 95.5% and 99.7%.

Note S4: Verification and demonstration of ACI-Km using virtual K_m-determination experiments

In one set of K_m-determination experiments, the enzyme at a constant concentration E_0 is mixed with its substrate at varying concentrations of S_0 to allow enzymatic interactions and product formation. The reaction progress curve, showing product concentration (P) versus reaction time, is recorded to determine the initial reaction velocity (v_0). Then, the Michaelis-Menten (MM) plot "v_0 vs S_0" is analyzed to determine $K_{m,det}$.

We used the Python program rankingKmSim.py to model the K_m-determination process. In the set of simulations, we set $k_1 = 100\ \mu M^{-1}s^{-1}$, $k_{-1} = 1\ s^{-1}$, and $k_2 = 99\ s^{-1}$, resulting in $K_m = (k_2 + k_{-1})/k_1 = 1\ \mu M$. 1% random noise was added to the product concentrations in the generated data. For each set of progress-curve simulations, the nominal total substrate concentration (S_0) ranged from 1000 to 0.01 μM, decreasing in 3-fold increments to generate eleven progress curves of "P vs time". Ten sets of simulations were performed with nominal total enzyme concentrations (E_0) fixed at 0.005, 0.01, 0.05, 0.1, and 0.5 μM. Each nominal E_0 value corresponded to two specific combinations of systematic errors in E_0 and S_0: one where $\Delta E_0/E_0 = 0.2$ and $\Delta S_0/S_0 = -0.2$, and another where $\Delta E_0/E_0 = -0.2$ and $\Delta S_0/S_0 = 0.2$. For instance, when the nominal E_0 was set to 0.01 μM, two sets of progress curves were simulated: in one case, the inputted true E_0 was set as 0.012 μM and the inputted true S_0 varied from 800 to 0.008 μM, reflecting relative systematic errors of $\Delta E_0/E_0 = 0.2$ and $\Delta S_0/S_0 = -0.2$. In the other case, the inputted true E_0 was set as 0.008 μM, and the inputted true S_0 varied from 1200 to 0.012 μM, reflecting relative systematic errors of $\Delta E_0/E_0 = -0.2$ and $\Delta S_0/S_0 = 0.2$.

In the following, we demonstrate the process of simulating progress curves and performing downstream data analysis for a specific case: nominal $E_0 = 0.01$ μM, nominal S_0 ranging from 1000 to 0.01 μM, with $\Delta E_0/E_0 = 0.2$ and $\Delta S_0/S_0 = -0.2$. The procedures for numerical simulations and data analysis in the other nine cases followed a similar approach. As described in the previous paragraph, introducing a relative systematic error of $\Delta E_0/E_0 = 0.2$ to the nominal E_0 and $\Delta S_0/S_0 = -0.2$ to the nominal S_0 resulted in true $E_0 = 0.012$ μM and true S_0 ranging from 800 to 0.008 μM (11 different concentrations). These "true" values were used as inputted parameters in the rankingKmSim.py program. Representative simulated progress curves are shown in Figure S1A. The linear regions of these 11 progress curves, corresponding to the 0.06–0.14 s time range, were analyzed using linear fitting to determine the initial reaction velocity (v_0) for each

nominal S_0. Representative linear analyses are presented in Figure S1B, and the resulting MM plot, "v_0 vs nominal S_0", for nominal E_0 = 0.01 μM is shown in Figure S1C. The ACI-Km program automatically and internally converts the dataset of "v_0 vs nominal S_0" into the binding isotherm "R vs nominal S_0" (Figure S1D) to calculate the PCI and ACI of K_m at various confidence levels.

In our previous work (Wang et al., 2024),[2] we demonstrated that the true input value of K_m should lie near one boundary of the computed ACI for K_m at a 68.3% confidence level when $\delta E_0/E_0 = |\Delta E_0/E_0|/1.36$ and $\delta S_0/S_0 = |\Delta S_0/S_0|/1.36$ are used as inputs in the ACI-Km program. To verify the ACI-Km program and its associated web application (https://aci.sci.yorku.ca), we input the following parameters into the web app: nominal E_0 = 0.01, $\delta E_0/E_0 = 0.2/1.36 = 0.15$, $\delta S_0/S_0 = 0.2/1.36 = 0.15$, and the MM plot "$v_0$ vs nominal S_0" (generated from simulated reaction progress curves). The web app then calculated the PCI and ACI of K_m, producing a PDF report (Figure S2). As shown in the report, the true K_m = 1 μM is located at the lower boundary of the ACI of K_m at the 68.3% confidence level, consistent with the theoretical prediction. Verification was subsequently extended to nine additional simulated datasets with varied nominal E_0 values and different combinations of relative systematic errors in E_0 and S_0. A summary of the results from these validation processes, conducted using synthetic data, is presented in Figure 4 of the main text.

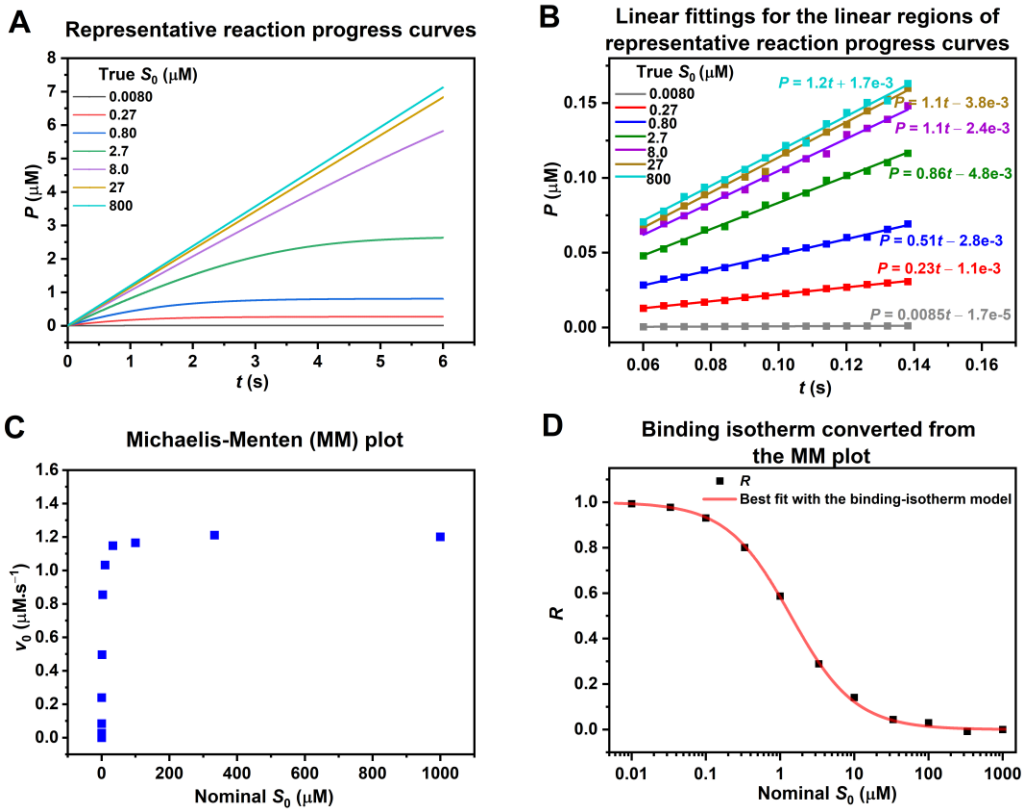

Figure S1. Virtual K_m-determination experiments and the downstream data analysis. **A)** Representative simulated enzyme–substrate reaction progress curves generated using the Python program rankingKmSim.py. **B)** Linear fits of the linear regions from the reaction progress curves shown in panel **(A)**. **C)** MM plot ("v_0 vs nominal S_0") derived from the analysis of the simulated reaction progress curves. **D)** Binding isotherm ("R vs nominal S_0") converted from the MM plot in panel **(C)** with the best fitting line using the binding-isotherm model (eq 15 in the main text). The R values were calculated using eq 14 in the main text by setting the v_0 obtained at the highest nominal S_0 as $v_{0,max}$. In this demonstration, the nominal E_0 was 0.01 μM, while the true E_0 was 0.012 μM, incorporating a relative systematic error of $\Delta E_0/E_0$ = 0.2.

ACI-Km Assessment

21/01/2025 11:31

Results: Confidence intervals of precision and accuracy of K_m with different confidence levels

	Confidence levels		
	68.3%	**95.5%**	**99.7%**
Precision confidence interval of K_m (PCI)	1.3–1.3 μM	1.3–1.3 μM	1.3–1.3 μM
Accuracy confidence interval of K_m (ACI)	1–1.6 μM	0.85–1.7 μM	0.67–1.9 μM

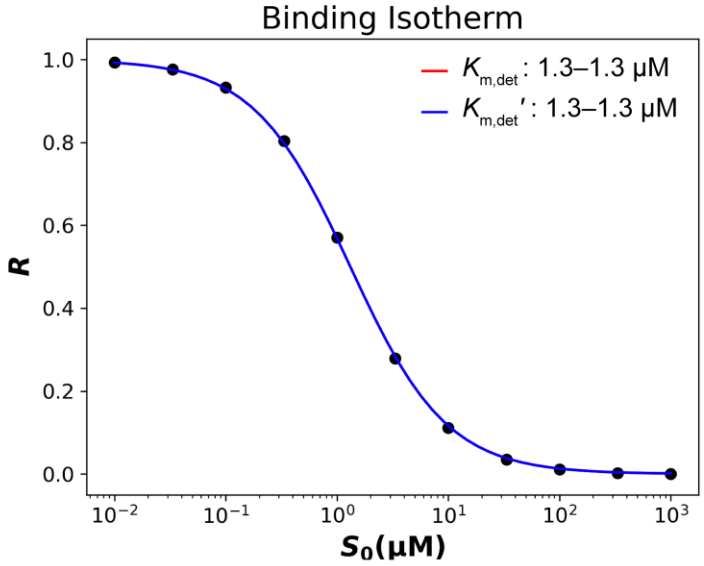

Input Data of MM plot

(E_0 = 0.01 μM)

S_0 (μM)	v_0 values
0.0	0.0
0.01	0.0085
0.033333	0.0279
0.1	0.0802
0.33333	0.2332
1.0	0.5089
3.33333	0.8559
10.0	1.0543
33.3333	1.1449
100.0	1.1733
333.3333	1.1836
1000.0	1.1865

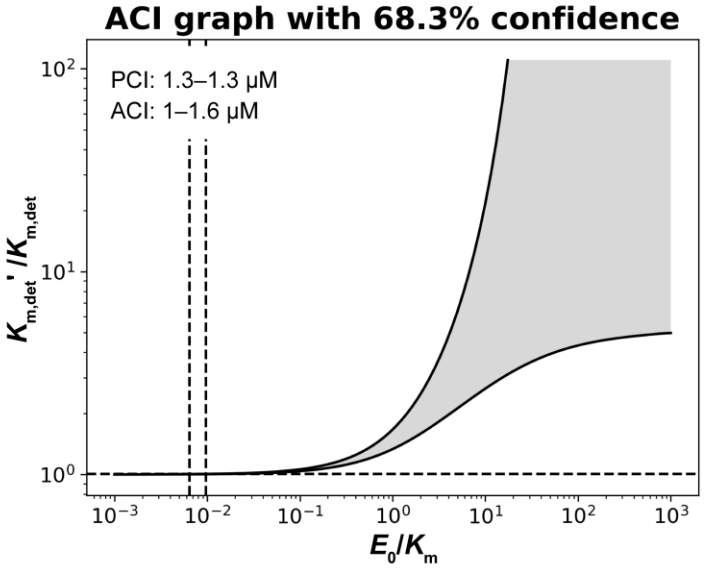

Figure S2. Example of a PDF report generated by the ACI-Km webapp (https://aci.sci.yorku.ca).

Note S5: Calculation of the ACI of K_m at low E_0/K_m ratio

Since the sensitivity of $K_{m,det}$ to E_0 values used in data fitting is insufficient for performing the proposed regression-stability test when $E_0/K_m < 0.001$, an alternative approach is needed to compute the ACI of K_m for very small E_0/K_m values. Based on eq S4 and eqs 10 and 12 in the main text, we infer that for very small E_0/K_m values, the contributions of systematic errors in E_0 and E_0/K_m to the systematic error of $K_{m,det}$ are negligible.

If we assume R values are only subject to random errors with no systematic error ($r = 0$), then the systematic error in $K_{m,det}$ is solely determined by the systematic error in S_0. This implies that for extremely small E_0/K_m values, the ACI of K_m can be defined by errors in S_0 alone. Without contributions from E_0/K_m or systematic error in E_0, we propose that the ACI of K_m can be estimated as $[K_{m,det}(1 - N\delta S_0/S_0), K_{m,det}(1 + N\delta S_0/S_0)]$, where N takes values of 1.36, 2.27, and 3.18 for confidence levels of 68.3%, 95.5%, and 99.7%, respectively.[2]

To validate this proposition, we investigated the ACI of K_m for E_0/K_m values ranging from 0.005 to 0.01 in increments of 0.001. Using the method described in Note S4, we simulated reaction progress curves for these E_0/K_m values while introducing two specific combinations of systematic errors: (*i*) $\Delta E_0/E_0 = 0.2$, $\Delta S_0/S_0 = -0.2$ and (*ii*) $\Delta E_0/E_0 = -0.2$, $\Delta S_0/S_0 = 0.2$. From these simulated reaction progress curves, we derived the corresponding MM plots ("v_0 vs S_0") and analyzed them using the ACI-Km webapp.

First, we confirmed that the computed ACI of K_m using $\delta E_0/E_0 = \delta S_0/S_0 = 0.15$ was identical to that obtained when only $\delta S_0/S_0 = 0.15$ ($\delta E_0/E_0 = 0$). This confirmed that the contribution of $\delta E_0/E_0$ to the ACI of K_m at very low E_0/K_m is negligible. Next, we compared the computed ACI of K_m with the proposed formula, $[K_{m,det}(1 - N\delta S_0/S_0), K_{m,det}(1 + N\delta S_0/S_0)]$ for the confidence levels mentioned above (Figure S3). The results in Figure S3 demonstrate strong consistency with our hypothesis, indicating that the ACI of K_m for low E_0/K_m (< 0.01) can be reliably computed using this alternative approach.

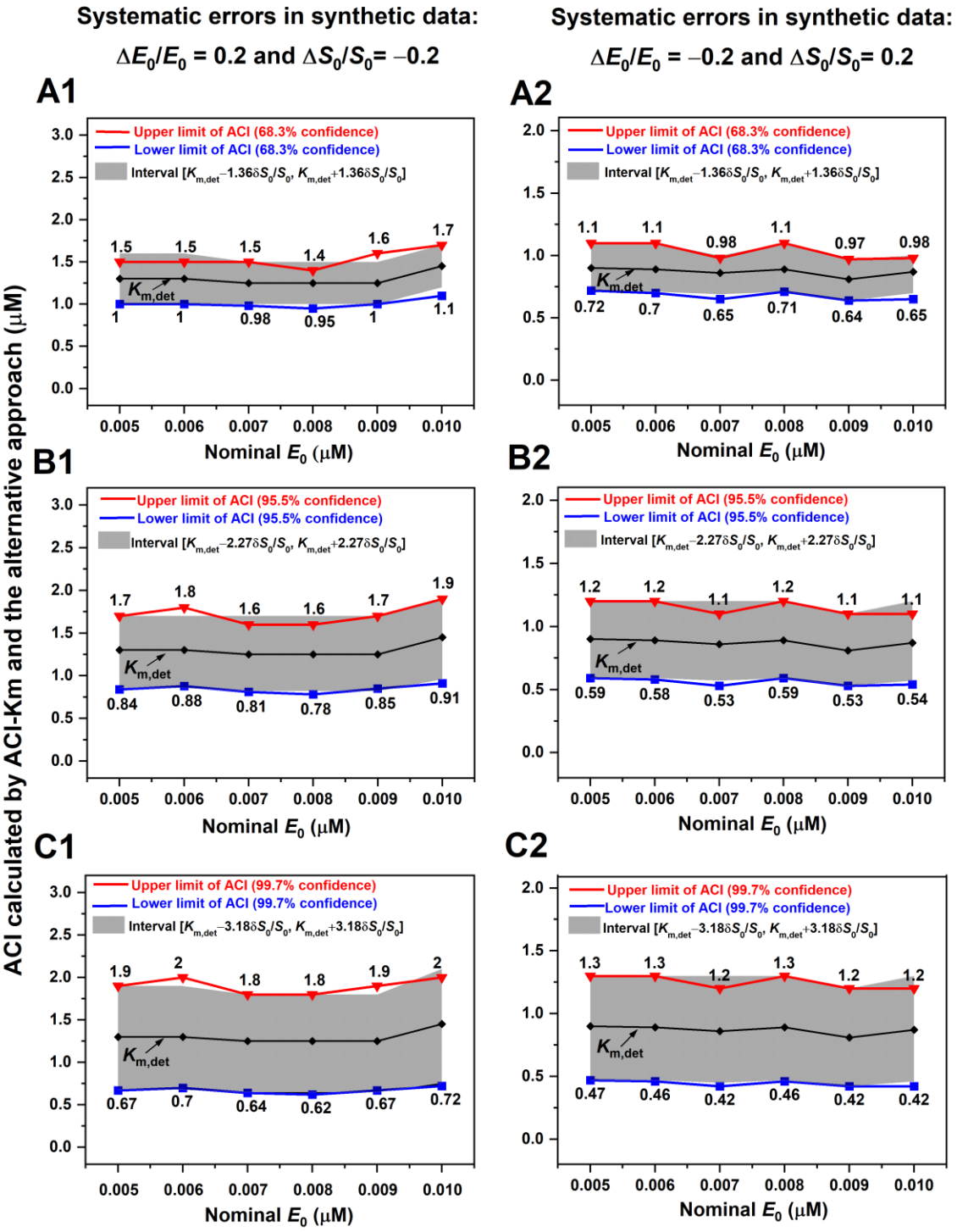

Figure S3. Comparison of ACI calculated using ACI-Km and the proposed alternative approach. The ratio of nominal E_0 to the true K_m values was varied from 0.005 to 0.01 in increments of 0.001. Two different combinations of systematic errors were introduced into the synthetic data: **A1, B1, C1)** $\Delta E_0/E_0 = 0.2$ and $\Delta S_0/S_0 = -0.2$, and **A2, B2, C2)** $\Delta E_0/E_0 = -0.2$ and $\Delta S_0/S_0 = 0.2$. Results were analyzed for three confidence levels: 68.3% **(A1, A2)**, 95.5% **(B1, B2)**, and 99.7% **(C1, C2)**.

Note S6: Data analysis for the K_m-determination experiment

Here, we demonstrate the data analysis process for the K_m-determination experiment using a nominal enzyme concentration of $[LDH]_0 = 0.87$ nM. In this experiment, the enzyme concentration was fixed at 0.87 nM, while the pyruvate concentration was varied from the lowest nonzero concentration of 23 μM to 2000 μM in 1.5-fold increments, resulting in 12 experimental reaction progress curves. Representative reaction progress curves are shown in Figure S4A. The linear regions of these 12 experimental progress curves, corresponding to the time range of 0–250 s, were analyzed using linear fitting to determine the initial reaction velocity (v_0) for each nominal $[pyruvate]_0$. Representative linear fits are presented in Figure S4B, and the resulting data points of "v_0 vs $[pyruvate]_0$" are shown in Figure S4C, including one data point with $v_0 = 0$ s^{-1} at $[pyruvate]_0 = 0$ nM.

The ACI-Km program automatically transforms the dataset of "v_0 vs $[pyruvate]_0$" into the binding isotherm "R vs $[pyruvate]_0$". Figure S4D illustrates the binding isotherm derived from the experimental "v_0 vs $[pyruvate]_0$" data points, along with the fitting line generated using the binding isotherm model (eq 8 in the main text). In this study, reaction progress curve measurements were performed in triplicate under identical conditions. Based on the linear fitting results of the triplicate progress curves, the average v_0 (along with its associated uncertainty) for each $[pyruvate]_0$ was calculated to construct the experimental MM plot, "average v_0 vs $[pyruvate]_0$" (Figure 5A in the main text). This MM plot was then automatically converted to a corresponding binding isotherm "average R vs $[pyruvate]_0$" (Figure 5B in the main text) by the ACI-Km program (https://aci.sci.yorku.ca) to compute the PCI and ACI of K_m for various confidence levels. The raw experimental data are provided in the supplementary file "Experimental_data.xlsx" (https://doi.org/10.6084/m9.figshare.26961733).

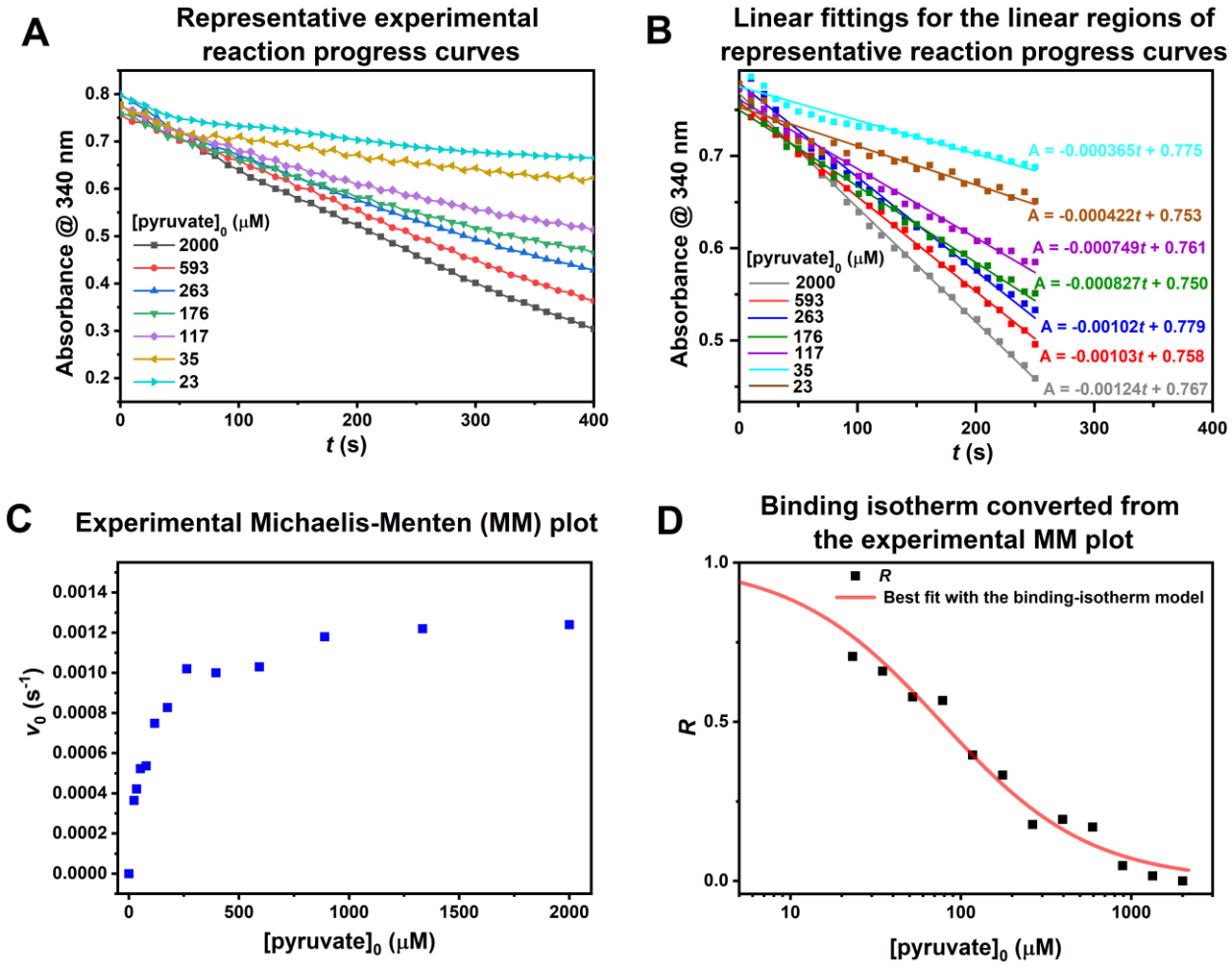

Figure S4. Illustration of the data-analysis process for a K_m-determination experiment in the LDH–pyruvate system. **A)** Representative experimental reaction progress curves. **B)** Linear fits of the linear regions (for time period 0–250 s) from the reaction progress curves shown in panel **(A)**. **C)** Data points of the MM plot ("v_0 vs [pyruvate]$_0$") derived from the analysis of the reaction progress curves. **D)** Binding isotherm "R vs [pyruvate]$_0$" generated from the MM plot in panel **(C)**, along with the best-fit line obtained using the binding isotherm model (eq 8 in the main text). The R values were calculated using eq 7 in the main text by setting the v_0 determined at the highest [pyruvate]$_0$ as $v_{0,max}$.

References

[1] T. Y. Wang, H. Ji, D. Everton, A. T. Le, S. M. Krylova, R. Fournier, S. N. Krylov, *Anal. Chem.* **2023**, *95*, 15826–15832.

[2] T. Y. Wang, J. Latimer, J.-L. Rukundo, I. Kogan, S. M. Krylova, S. Schreiber, P. Kohlmann, J. Jose, S. N. Krylov, *Precis. Chem.* **2025**, *3*, 89–104.

[3] ERROR PROPAGATION, https://www.chem.hope.edu/~polik/Chem345-2000/errorpropagation.htm (accessed August 26, 2024).

[4] M. Kanoatov, V. A. Galievsky, S. M. Krylova, L. T. Cherney, H. K. Jankowski, S. N. Krylov, *Anal. Chem.* **2015**, *87*, 3099–3106.

[5] T. Y. Wang, J.-L. Rukundo, Z. Mao, S. N. Krylov, *ACS Chem. Biol.* **2024**, *19*, 1852–1867.

[6] Z TABLE, https://www.ztable.net/contact/ (accessed September 6, 2024).